Addis Ababa University

School of Graduate Studies

Physicochemical Characterization of Native Cellulose and Microcrystalline Cellulose from Enset Fiber and Evaluation of Microcrystalline Cellulose as Directly Compressible Excipient

Sintayehu Alemu (B.Pharm)

July, 2019

Addis Ababa, Ethiopia

Physicochemical Characterization of Native Cellulose and Microcrystalline Cellulose from Enset Fiber and Evaluation of Microcrystalline Cellulose as Directly Compressible Excipient

A Thesis Submitted to Department of Pharmaceutics and Social Pharmacy, School of Pharmacy, College of Health Sciences, in Partial Fulfillment of the Requirements for the Degree of Master of Science in Pharmaceutics

Sintayehu Alemu (B.Pharm)

Advisers: Prof. Tsige Gebre-Mariam
Dr. Anteneh Belete

July, 2019

Addis Ababa, Ethiopia

Addis Ababa University

School of Graduate Studies

Physicochemical Characterization of Native Cellulose and Microcrystalline Cellulose from Enset Fiber and Evaluation of Microcrystalline Cellulose as Directly Compressible Excipient

By: Sintayehu Alemu (B.Pharm)

Approved by:

Name	Signature	Date
Prof. Tsige Gebre-Mariam (Advisor)	_____	_____
Dr. Anteneh Belete (Advisor)	_____	_____
Dr. Getahun Paulos (External Examiner)	_____	_____
Dr. Gebremariam Birhanu (Internal Examiner)	_____	_____

ACKNOWLEDGMENTS

First of all, I would like to express my heartfelt gratitude and appreciation to my advisors Prof. Tsige Gebre-Mariam and Dr. Anteneh Belete for their valuable guidance, useful suggestions, keen interest and constant encouragement.

I am also thankful for Mr. Tesfaye Gabriel for his inspiring and priceless cooperation, Mr. Fekade Tefera, for his support and encouragement during laboratory work and the staff members of the Department of Pharmaceutics and Social Pharmacy as well as Pharmaceutical Chemistry and Pharmacognosy for their respective support during my entire work.

I am highly grateful to the Ethiopian Pharmaceutical Manufacturing Share Company (EPHARM) for providing me access to their Fourier Transform Infrared (FTIR) spectroscopy and donating me Paracetamol powder, Mrs Munna Ahmed, Plant Manager, East Africa Pharmaceutical Manufacturing Share Company for allowing me access to their tablet compression machine, Chemical Engineering Department, Institute of Technology, AAU for the access to their spray dryer and Material Science Engineering Department, Adama Science and Technology University for providing access to X-ray diffractometer, Thermogravimetric and Differential Thermal Analysis Apparatus, Ethiopian Public Health Institute for providing access to their Furnace and Ethiopian Leather Industry Development Institute for providing access to Scanning electron microscope (SEM).

I also would like to acknowledge Addis Ababa University and Jimma University for sponsoring my study.

Table of Contents

LIST OF TABLES

LIST OF FIGURES

ACRONYMS AND ABBREVIATIONS

AA: Acetic Acid

API: Active Pharmaceutical Ingredients

BP: British Pharmacopoeia

CI: Compressibility Index

CrI: Crystallinity Index

DC: Direct Compression

DP: Degree of Polymerization

DSC: Differential Scanning Calorimetry

DTA: Differential Thermal Analysis

DTG: Derivative Thermogravimetry

DVS: Dynamic Vapor Sorption

Ef-C: Enset fiber cellulose

Ef-MCC: Enset fiber microcrystalline cellulose

Ef-MCC-mod: Mechanically agitated and oven dried Ef-MCC

Ef-MCC-od: Oven dried enset fiber microcrystalline cellulose

Ef-MCC-sd: Mechanically agitated and spray dried Ef-MCC

FA: Formic Acid

FTIR: Fourier Transform Infrared

HR: Hausner Ratio

IR:	Infra-Red
LSR:	Lubricant Sensitivity Ratio
MCC:	Microcrystalline Cellulose
PAA:	Peroxyacetic Acid
PFA:	Peroxyformic Acid
RH:	Relative Humidity
TA:	Thermal Analysis
TGA:	Thermogravimetric Analysis
USP:	United State Pharmacopoeia
XRD:	X-ray Diffraction

ABSTRACT

Cellulose is naturally occurring polymer on earth and it is obtained from wood, cotton, agricultural residues and different fibrous plants. Enset (*Ensete ventricosum*) is a plant indigenous to Ethiopia. It is serves as food, forage, fiber and medicinal uses. Enset fiber is a rich source of cellulose. The aim of this study was to extract and characterize native cellulose and microcrystalline cellulose (MCC) from enset fiber and evaluate MCC as directly compressible excipient. Cellulose was extracted by using formic acid/acetic acid (at 70:30 ratio). Different enset fiber MCCs were prepared by using hydrochloric acid. The proximate yield of enset fiber cellulose (Ef-C) and enset fiber microcrystalline cellulose (Ef-MCC) were found to be 56.97% and 65.42-82%, respectively. The degree of polymerization (DP) of Ef-MCC powders were less than 350. Fourier Transform Infra-red spectra (FT-IR) of Ef-MCCs indicated the typical absorption peaks of cellulose.

The physicochemical studies of Ef-MCCs revealed, moisture content of <7% w/w, bulk densities 0.24, 0.33 and 0.27 gm/cm^3 for oven dried Ef-MCC (Ef-MCC-od), mechanically agitated oven dried Ef-MCC (Ef-MCC-mod) and spray dried Ef-MCC (Ef-MCC-sd), respectively. Ash value (0.03), pH (6.76), water soluble substances (0.17%) and ether soluble substances (0.046%) of Ef-MCCs were all within the allowable limit of USP 30/NF 25.

Laser diffraction studies showed that Ef-MCCs had normal size (log) distribution with a mean particle size ranging between 57-79 µm. Crystallinity index (CrI) of Ef-C was 78.5% while the CrI of Ef-MCCs was 85-89%. Scanning electron microscopy (SEM) also showed Ef-MCC had little aggregates of particles, rod-shaped, rough surface morphology and shorter fiber strands.

Ef-MCC-mod successfully accommodated 50% paracetamol whereas Ef-MCC-sd up to 65%. Disintegration time and *invitro* drug release of paracetamol tablets were also within USP 30/NF 25 specification. EF-MCCs, especially, Ef-MCC-sd can be considered as a potential alternative excipient since they exhibited similar characteristics with Avicel PH101.

Keywords: Cellulose, Dilution potential, Enset, Enset fiber, Microcrystalline cellulose.

1. INTRODUCTION

1.1. Cellulose

The name cellulose was coined in 1839 by Anselme Payen, French agricultural chemist, when he conducted systematic study of cellulose chemistry during 1837-1842 and hence entitled "Father of Cellulose Chemistry." He showed that plant tissue, cotton linters and various leaves yielded a resistant fibrous substance when purified by acid-ammonia treatment followed by extraction with water, alcohol and ether. He arrived at the conclusion that the fibrous substance of plant cells consists of one uniform chemical substance: a carbohydrate composed of glucose residues (Mertens, 2003; Klemm *et al*., 2005).

Cellulose is the most abundant naturally occurring polymer on earth and the most common organic polymer (biopolymer) in nature (Bhattacharya *et al*., 2008; Figueiredo *et al*., 2010; Haafiz *et al*., 2013). Its molecular structure (Figure 1) implies a repeating unit of linear polymer of β-D-glucopyranose (β-D-Glcp) that is covalently linked through acetal functional group between the OH of C-4 of one glucopyranose unit and the C-1 of the next glucopyranose unit via glycosidic bond (β-1,4-glucan) (Klemm *et al*., 2005; Figueiredo *et al*., 2010).

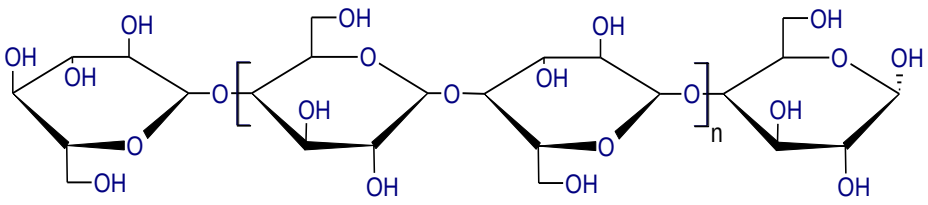

Figure 1: Molecular Structure of Cellulose.

Cellulose is eco-friendly and biocompatible for the production of green products. Thus, producing new sustainable and eco-friendly materials has gained the attention of researchers worldwide (Maepa *et al*., 2015; Krstic *et al*., 2018).

Cellulose exhibited four polymorphs i.e., cellulose I, II, III and IV. Cellulose I is the form found in nature. It has been found to be a mixture of two polymorphs collectively known as native cellulose (I_α and I_β). Cellulose I_α is dominantly produced by primitive organisms such as bacteria and algae while cellulose I_β is produced by the higher plants (Sugiyama *et al*., 1991a; Saxena

and Brown, 2005). In cellulose I, the chains are all oriented in the same direction (parallel). Cellulose II is formed when the lattice of cellulose I is destroyed either by **swelling** with strong alkali or by dissolution. In cellulose II, the chains are oriented antiparallel (opposite direction). Treatment of cellulose I and cellulose II with liquid ammonia gives cellulose III form and the heating of cellulose III generates cellulose IV form. However, some authors consider that cellulose III and cellulose IV crystalline are not true polymorphic forms, but are rather disordered versions or mixtures of celluloses I and II (Figueiredo *et al*., 2010). Cellulose is known to be insoluble in water and most organic solvents and their poor solubility is attributed primarily to the strong intramolecular and intermolecular hydrogen bonding between the individual chains (Lin *et al*., 2009; Gbenga and Fatimah, 2014). With extensive efforts, cellulose has found to be effectively dissolved in several solvents and Cupper-ammonium hydroxide solution is among common solvents (Karande *et al*., 2011; Zhong *et al.,* 2013*).*

1.2. Sources of Cellulose

The growing demand for environmental sustainability has encouraged research into biodegradable polymers to minimize the environmental impact of conventional polymers. In this context, plant fibers are an attractive material as they constitute rich sources of cellulose, the main component of plant cell walls (Tibolla *et al*., 2014).

The primary occurrence of cellulose is lignocellulosic materials in forests, with wood as the most important source. Lignocelluloses are composed of cellulose, hemicellulose and lignin. Other cellulose-containing materials include cotton, hemp, agriculture residues, water plants, grasses and other plant substances. Commercial cellulose production concentrates on harvested sources such as wood or on naturally highly pure sources such as cotton (Klemm *et al*., 2005; Maiti *et al*., 2013).

The chemical analysis of different plant fiber revealed different yields of cellulose. The study conducted on corn stover fiber shows that 45.5% of the fiber composition is cellulose (Costa *et al*., 2013). Cotton stalk contains 87.52% cellulose (Zhang *et al*., 2011). The extracts of jute fibers yield 59.8% of cellulose (Jahan *et al*., 2011).

1.3. Cellulose from Enset (*Ensete ventricosum*) Fiber

Enset (*Ensete ventricosum*) (Figure 2 a) is a plant indigenous to Ethiopia, closely related to the banana tree. Because it resembles the banana tree, but does not produce banana, enset is often referred as “False Banana" (Gebre-Mariam and Schmidt., 1996a).

Enset is perennial, herbaceous plant with long broad leaves which belongs to a Family Musaceae. It is a multi-purpose root crop and widely grown in central, south and south western part of Ethiopia for its food, forage, fiber and medicinal uses. This crop contributes to food security (a traditional staple food crop) for more than 20% of Ethiopia’s population notably southern and southwestern parts of Ethiopia (Gebre-Mariam and Schmidt., 1996a; Yemataw *et al*., 2014; Lemma *et al*., 2016). Enset can be grown everywhere in Ethiopia. Naturally, it can adapt a wide range of geographical location with altitude ranged from 100 to 3100 meters above sea level. However, it grows best at elevations between 1800 m and 2450 meters. Enset based farming system is an indigenous and sustainable agricultural system that covers large hectares of land assumed to be covered with enset cultivation in Ethiopia (Magule *et al*., 2014).

(a) (b)

Figure 2: Enset plant (a) and enset fibers (b).

The fiber (Figure 2b), with a hair like structure, locally called “*kacha*” is collected after scarping of the leaf sheath and leaf bases around the pseudo stem. It is main solid residues which is produced as byproduct during for enset based foods preparation. This is abundant natural

resource and can be potential source of cellulose (Lemma *et al*., 2016) and is also potential cellulosic source in making MCC.

1.4. Extraction of Cellulose from Lignocellulosic Materials

The cellulose chains are packed into microfibrils which are stabilized by hydrogen bonds. These fibrils are attached to each other by hemicelluloses and amorphous polymers of different sugars as well as other polymers such as pectin and covered by lignin (Figure 3). Hemicellulose has a lower molecular weight than cellulose and is composed of mainly pentoses (like xylose and arabinose) and hexoses (like mannose, glucose, and galactose). It also has considerable side chain branching consisting of hydrolysable polymers. Lignin is a complex, crosslinked, three-dimensional polymer formed with phenylpropane units. It is an amorphous polymer whose attributes include providing rigidity to the plant cell wall and resistance against microbial attack (Mosier *et al.*, 2005; Carrier *et al.*, 2011).

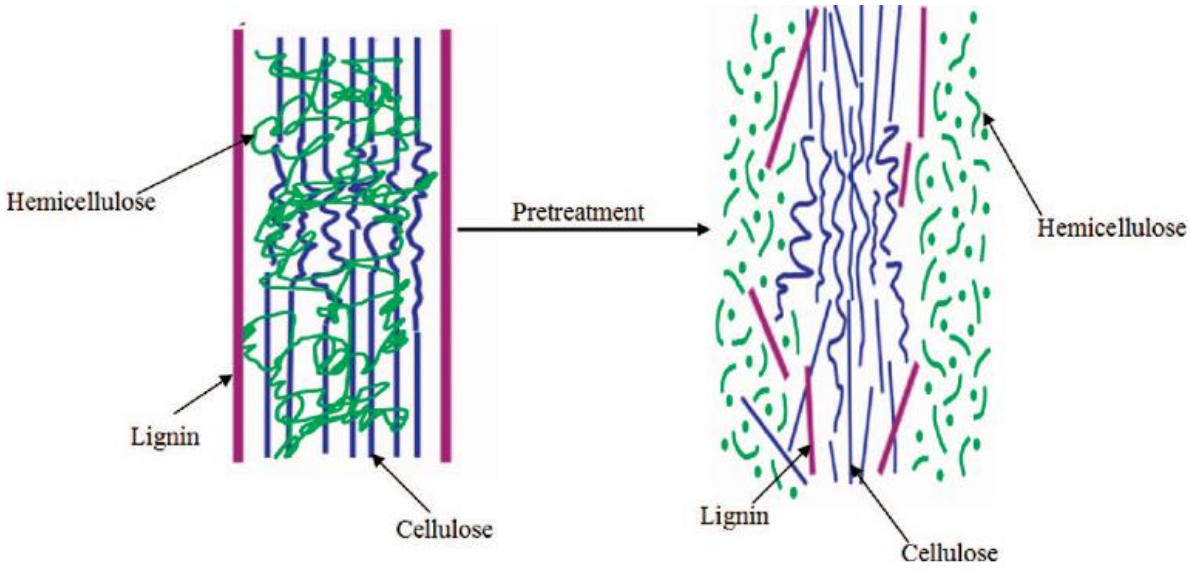

Figure 3: Schematic representation (adapted from Mosier *et al*., 2005) of the matrix of polymers in which cellulose exists.

Pretreatment is required to alter the structure of cellulosic materials to make cellulose more accessible to reactants. The pretreatment of biomass by different methods removes hemicellulose and lignin from polymer matrix (Mosier *et al.*, 2005; Adel *et a*l., 2010). Thus, the goal of the pretreatment process is to remove lignin and hemicellulose and increase the porosity

of the lignocellulosic materials. Pretreatment technologies are usually classified into physical, chemical, physicochemical (steam explosion), biological or a combination of these. Biological pretreatment involves the use of microorganisms (mainly fungi) to degrade lignin and hemicellulose but leave the cellulose intact (Kumar and Wyman, 2009; Sanchez, 2009; Shi *et al*., 2008). Even though biological pretreatments involve mild conditions and are of low cost, the disadvantages are the low rates of hydrolysis and long pretreatment times required compared to other technologies (Sun and Cheng, 2002).

1.4.1. Physical pretreatment

Physical pretreatment methods, including mechanical operations, irradiation and ultrasonic pretreatment, have been utilized to enhance the accessibility of hydrolysable polymers within lignocellulosic material. Among the physical pretreatments, mechanical pretreatment is widely used for waste materials, such as agricultural residues or any other crops and forestry residues (Amin *et al*., 2017). Mechanical pretreatment such as chipping, grinding and/or milling can be applied to reduce size of materials (Kumar *et al*., 2009) so that it facilitates accessibility of cellulose.

1.4.2. Chemical pretreatments

Alkaline: Alkaline pretreatment involves the use of bases, such as sodium, potassium, calcium, and ammonium hydroxide for the pretreatment of lignocellulosic biomass. The use of an alkali causes the degradation of ester and glycosidic side chains resulting in structural alteration of lignin, cellulose swelling and partial decrystallization of cellulose (Cheng *et al*., 2010; Ibrahim *et al*., 2011; McIntosh and Vancov, 2010). Sodium hydroxide has been extensively used and it has been shown to disrupt the lignin structure of the biomass, increasing the accessibility of cellulose and hemicellulose (Zhao *et al*., 2008).

Acid: Acid pretreatment involves the use of concentrated and diluted acids to break the rigid structure of the lignocellulosic material. Due to the ability to remove hemicellulose, acid pretreatments have been used as parts of overall processes in fractionating the components of lignocellulosic biomass (Sassner *et al*., 2008). The acetic acid or formic acid process is an effective alternative method to fractionate lignocellulosic materials to produce cellulose.

Organic solvent (acetic acid/formic acid) cleaves ether bonds between lignin and hemicellulose, thereby accelerating the delignification process. The method has been used to separate cellulose, hemicellulose and lignin from lignocellulosic materials with efficient chemical recovery (Jahan *et al.*, 2011; Jahan *et al*., 2014).

1.5. Modification of Cellulose

Cellulose can be transformed into materials in the micro- and nanoscale range by various treatments. These can be by physical modification (e.g. MCC), chemical modification (e.g. ethyl cellulose, hydroxyethyl cellulose, hydroxypropyl cellulose and carboxymethyl cellulose), enzymatic or mechanical treatments. The modified cellulose can be used in several fields e.g. in pharmaceuticals and for food and paper applications. Modification of cellulose is performed to improve processability and to produce cellulose derivatives (cellulosic) which can be tailored for specific industrial applications (Shokri and Adibkia, 2013; Jedvert and Heinze, 2017).

1.6. Microcrystalline Cellulose

MCC is partially depolymerized cellulose prepared by treating cellulose obtained as a pulp from fibrous plant material with mineral acids (Wang *et al.,* 2010; Setu *et al*., 2014). MCC is defined by a Degree of polymerization (DP) less than 350 glucose units, compared to DPs in the order of 10,000 units for the original native cellulose. Accordingly, it is merely an identity test to distinguish MCC from cellulose (Thoorens *et al*., 2014). It occurs as a fine white, odorless, crystalline powder, which is insoluble in water, dilute acids and alkali and common organic solvents (Suzuki *et al*., 1999; Das *et al.,* 2010; Wang *et al.*, 2010).

MCC was introduced in the 1950s and commercialized as Avicel® PH in 1962 (Thoorens *et al*., 2014). In 1964, Avicel® PH was introduced to the pharmaceutical industry as an ingredient for direct compression tableting (Albers *et al*., 2006).

MCC has high tensile strength which is better than most of the reinforcers used in polymer composite manufacturing. For instance, MCC was acetylated with ketene and vinyl acetate, respectively, for the preparation of MCC-reinforced polyethylene composites. Polypropylene composites reinforced with MCC were developed by using maleic anhydride (Liu *et al*., 2017). It also poses excellent properties such as renewability, low density, high surface area, stability,

inertness, biodegradability and higher mechanical properties which make it as alternative filler in the composite preparation and a good candidate in the manufacturing of biodegradable polymer composites (Sundar, 2011).

MCC is mostly derived from numerous sources such as cotton and wood pulp, bamboo, viscose rayon, newsprint waste, hosiery waste as well as agricultural residues including sugarcane bagasse, rice straw, cotton stalks and soybean husk by hydrolysis of cellulose (Wang *et al.*, 2010; Kambli *et al*, 2017). The hydrolysis of cellulose to obtain MCC can be accomplished using mineral acid, enzymes or microorganisms. Although enzymatic methods are desirable because glucose, a useful by-product, is created, these methods are more expensive and create MCC products having a lower crystallinity. Thus, acid hydrolysis is the conventional method of choice for manufacturing MCC (Adel *et al.*, 2011). In the process of acid hydrolysis of purified cellulose for making MCC, the non-crystalline region (amorphous area) is preferentially hydrolyzed, dissolved and removed while the cellulose crystals are recovered (Wang *et al.*, 2010; Terinte *et al*., 2011; Kambli *et al*, 2017).

Though there are various sources for preparing pharmaceutical-grade MCC, there is a constant search for new sources of MCC because of the high cost of commercially available products (Bhimte and Tayade., 2007).

1.7. Application of Cellulose and Microcrystalline Cellulose

Cellulose is widely used in a variety of commercial applications in the food, textile, paper and pharmaceutical industries due to its high availability and attractive chemical and physical properties such as biocompatibility, biodegradability, thermal and chemical stability (Bochek, 2003; Oliveira *et al*., 2011; Maheswari *et al*., 2012; Zhong *et al.*, 2013). However, cellulose has some inherent drawbacks. These include poor solubility in common solvents, lack of thermoplastic properties, high hydrophilicity and lack of antimicrobial properties. To overcome such drawbacks, the controlled physical and/or chemical modification of the cellulose structure is necessary (Roy *et al*., 2009). The production of cellulose derivatives broadens the applications of cellulose by modifying the polymer chemically or physically in terms of hydrophobicity, processability and solubility. For application as excipient in pharmaceutical industry, an important aspect is the improvement in processability of cellulose; in this sense, the most

important cellulose derivative is MCC (Oliveira *et al*., 2011). MCC has been used for many years in different industries like cosmetics, plastics, food, pharmaceuticals etc. because of its excellent properties (Das *et al.,* 2010).

1.7.1. Pharmaceutical Application of Microcrystalline Cellulose

Because of its chemical inactivity, absence of toxicity, high sorption and great hygroscopicity, MCC has received great interest in pharmaceutical formulations (Trache *et al*., 2014). It is a widely used tableting excipient. In terms of tableting technology, the material is described as filler-binder in that it is usually added to formulations to enhance compactibility (Edge *et al*., 2000). It is widely used as thickener and viscosity enhancer in liquid dosage forms and also enhances flowing property in solid dosage forms (Ibrahim *et al.,* 2013; Wang *et al.,* 2010).

There has been enormous interest in producing MCC for pharmaceutical use because of its high compactness under minimum compression pressures, high binding capability and ability to prepare tablets that are extremely hard, stable, yet disintegrate rapidly. All these properties make MCC particularly valuable as a filler and binder for tablet formulations prepared by direct compression (DC). In addition to its use in DC formulations, MCC is used as a diluent in tablets prepared by wet granulation as well as a filler for capsules and spheres (Setu *et al*., 2014).

1.7.1.1.Microcrystalline cellulose as direct compressible excipient

DC tableting is the most economical technique in the production of large number of tablets. It is a continuously growing field in tablet manufacture (Nada and Graf, 1998; Alfa *et al*., 2017). MCC is regarded as the best excipient for DC tableting (Bhimte and Tayade., 2007) and it is one of the mostly used filler-binders in direct tablet compression. The excipients for DC are in most cases modified natural products. Excipients of organic origins are developed from various natural resources and amongst them, cellulose is the most popular one. MCC is among currently marketed DC excipients. Excipients from plant sources are generally nontoxic and renewable means for the sustainable supply of less expensive pharmaceutical excipients (Chirayil *et al*., 2014).

MCC popularity in DC is due to its excellent binding properties when used as a dry binder. It also works as a disintegrant and lubricant and has a high dilution potential in DC formulations.

Dilution potential is the amount of poorly compressible drug that can be satisfactorily compressed into a tablet with a given DC excipient (Gohel and Jogani, 2005; Olowosulu *et al*., 2014). A DC excipient should have high dilution potential so that the final dosage form has a minimum possible weight (John *et al.*, 2013). Low bulk density MCC will have a higher dilution potential and may better counteract the poor tableting properties of APIs (Pönni *et al*., 2012).

The dilution capacity is certainly an important characteristic of a direct tableting excipient. A direct tableting excipient has the ability to incorporate a certain amount of a poorly compactable drug. The dilution capacity is understood as a critical value of the mass fraction above which the compactibility of the tableting mixture vanishes (Kuentz and Leuenberger, 2000). When a certain dilution value is reached the direct tableting agent can no longer become compact; this value corresponds to the dilution potential of that agent (Beten *et al*., 1994). MCC possesses almost ideal properties as it is highly compressible with maximum dilution potential, self-lubricating, glidant and disintegrant. Therefore, MCC has been used successfully for DC with many drugs, including critical examples like pancreatin, paracetamol, hydrochlorothiazide and ascorbic acid (Nada and Graf, 1998).

MCC can be used as an anti-adherent (5–20%), a disintegrant (5–15%) and as a diluent (20–90%) (Rowe *et al.*, 2006). However, many authors studied the plasto-elastic behavior of paracetamol-MCC mixtures and pointed out the optimum concentration of MCC as ranging between 25 and 50% in order to compress into satisfactory tablets as far as tensile strength, friability and capping tendency were concerned (Bangudu and Pilpel, 1984; Yu *et al.*, 1988; Nada and Graf, 1998). Capping occurred when the amount of Avicel in paracetamol fell below 25% w/w (Yu *et al.*, 1988) and concentration above 25% prevent capping and lamination in paracetamol tablets (Nada and Graf, 1998). Direct compression uses more than 30% of the drug in the formulation, mainly for drugs that present poor flowability (Martinello *et al.*, 2006). Hence, for better evaluation of direct compressibility of MCC, due attention was given for drug with inherent difficulties in tablet manufacture e.g. high dose level, poor compressibility and flowability.

1.7.2. Other application of microcrystalline cellulose

Apart from Pharmaceutical application, MCC is used in food industry as stabilizer, emulsifier, thickener and gelling agents in several dairy compounds. It has been also widely used in cosmetic and medical industries as a water-retainer and a reinforcing agent in composite (El-Sakhawy *et al*., 2006; Wang *et al.*, 2010).

2. SIGNIFICANCE OF THE STUDY

The consumption of cellulose for various industrial application is continuously increasing worldwide. As the major source of cellulose is wood (conventional sources), the increased consumption even in countries where wood resources are limited increases deforestation. With the increasing consumption of cellulose and its derivatives, it is becoming difficult to satisfy the large demand from conventional resources. Globally, the forest resources are diminishing while the demand of cellulose and cellulose derivatives is increasing. These issues enforce scientists to look for alternative fibrous resources especially non-wood one (Maheswari *et al*., 2012).

The high demand and importance of MCC used in pharmaceutical industries has led to the utilization of locally and naturally occurring materials in the production of MCC (Umeh *et al*., 2014). However, Ethiopian industries have relied on imported MCC of limited sources for use in various applications. This incurred large amount of foreign currency and this has led to the research for environmentally friendly and locally available sources of cellulose and cellulose derivatives such as MCC. Therefore, finding alternative cellulose sources, especially from abundantly available and renewable sources is highly valuable. MCC from enset fiber has not been reported. This study has investigated enset fiber as potential source of cellulose and MCC and evaluation of MCC as direct compressible excipient.

Thus, the study attempted to answer the following questions:

i) What is cellulose and MCC yield potential of enset fiber?
ii) Do Ef-MCC have similar characteristics with Avicel PH101?
iii) What is the direct compression property of MCC from enset fiber cellulose?

Avicel PH101 was used as standard with which the prepared MCC was compared. Moreover, paracetamol was used as a model drug for this study due to its poor compression ability, its tablets show a tendency to cap and it has elastic deformation characteristics (Martinello *et al.*, 2006).

3. OBJECTIVES

3.1.1. General Objective

- To extract and characterize native cellulose and microcrystalline cellulose from enset fiber and evaluate microcrystalline cellulose as directly compressible excipient.

3.1.2. Specific Objectives

- To extract and characterize cellulose from enset fiber;
- To prepare and characterize MCC from native enset cellulose; and
- To evaluate enset fiber MCC as directly compressible excipient.

4. EXPERIMENTAL

4.1. Raw Materials and Chemicals

Enset fiber (raw material) were collected from Woliso, Southwest Showa Zone, Oromia Region, Ethiopia. Acetic acid (99.9%) (Sigma Aldrich, Germany), Ammonium hydroxide (28%) and Hydrogen peroxide (30%) were obtained from Carlo erba (Farmatalia Carlo erba reagents S.P.A/Carlo erba reagents S.A.S, France), Avicel PH101, Copper sulphate(Pentahydrate, 98.5%), Formic acid (85%), Potassium iodide, Silica gel, Xylene and Zinc chloride were obtained from Loba Chem (Loba Chemie Pvt. Ltd, India), Diethyl ether (Central drug house Ltd, India), Hydrochloric acid (37%) (BDH Chemicals Ltd, England), Magnesium stearate (Bulvinos Chemicals Ltd, England), Sodium chloride (99.8) (UNI-CHEM), Sodium hydroxide (99.8%) (Alphax chemical industry, India) and Distilled water were used. Paracetamol powder was kindly donated by the Ethiopian Pharmaceutical Share Company (EPHARM).

4.2. Methods

4.2.1. Extraction of cellulose and preparation of microcrystalline cellulose

4.2.1.1. Extraction of cellulose

The method used by Jahan *et al.,* (2014) was employed for cellulose extraction. Accordingly, a mixture of 85% of formic acid and 99.5% acetic acid (at ratio of 70:30 by volume) was poured into the enset fiber in Erlenmeyer flask at a fiber to liquor ratio of 1:8 and treated at 100 ^{o}C in water bath for 1.5 h. Fibers were filtered and washed thoroughly with distilled water. In the next step, pulps were further delignified by treating with a mixture of Peroxyformic Acid/Peroxyacetic Acid (PFA/PAA) solution in water bath at 100 ^{o}C for 1.5 h at fiber to liquor ratio of 1:8. PFA/PAA solution mixture was prepared in 1:1:2 ratio of 85% FA/ 99.5% AA/10% H_2O_2. Finally, the delignified fibers were bleached by treating at 1:10 pulp to liquor ratio with 6% H_2O_2 and 4% NaOH solution mixtures in water bath at 100 ^{o}C for 1 h. The pulp was washed with distilled water and oven dried (KOTTERMANN 2711, Germany).

4.2.1.2. Preparation of microcrystalline cellulose

MCC was prepared by using the method developed by Battista (1950) and Battista and Smith (1962). Accordingly, 2.5M of HCl was heated to temperature of 100 ^{o}C on hotplate. Then, enset fiber cellulose (i.e., 1:20 fiber to liquor ratio) was added to the boiling acid and hydrolyzed for 30 min under stirring. The residue after hydrolysis was filtered and repeatedly washed with distilled water. The slurry was then treated with 5% ammonium hydroxide solution and thoroughly washed with distilled water until it was acid free. Subsequently, the slurry was processed in different ways: the first batch was oven dried (KOTTERMANN 2711, Germany) at 50 ^{o}C to dryness and denoted as Ef-MCC-od to mean oven dried enset fiber MCC. The second batch was mechanically agitated prior to drying and then oven dried under similar condition with the first batch. This batch was denoted as Ef-MCC-mod to mean mechanically agitated oven dried enset fiber MCC. After drying, both batches were pulverized using pulverisette (FRITSCH, Germany). The resulting powders were screened via 224 µm sieve. The third batch was mechanically agitated and spray dried using spray drier (Tall Form Spray Drier FT80, England) at inlet temperature of 175 ^{o}C, outlet temperature of 120 ^{o}C under air pressure of 1bar and denoted as Ef-MCC-sd to mean mechanically agitated spray dried enset fiber MCC.

4.2.1.3. Determination of percent yield

Percent yield of Cellulose was calculated using the following formula.

$$\%\text{Yield Cellulose} = \frac{\text{Weight of dry cellulose}}{\text{Original weight of dry fiber}} * 100 \ldots\ldots\ldots\ldots\ldots\ldots\ldots\ldots\ldots\ldots \text{Eq. 1}$$

Similarly, the percentage yield of Ef-MCC obtained from different batches was also determined.

$$\%\text{Yield MCC} = \frac{\text{Weight of dry MCC}}{\text{Original weight of Cellulose}} * 100 \ldots\ldots\ldots\ldots\ldots\ldots\ldots\ldots\ldots\ldots\ldots\ldots \text{Eq. 2}$$

4.2.2. Physicochemical characterization

4.2.2.1. Identification tests of cellulose and microcrystalline cellulose

The chemical identification was conducted as per USP (USP30/NF25, 2007). Accordingly, 10 mg of sample was dispersed in 2 ml of iodinated zinc chloride solution composed of 1.9 g/ml zinc chloride, 0.62 g/ml potassium iodide, 0.05 g/ml iodine and the color change observed when the sample came in contact with the solution.

4.2.2.2. Determination of degree of polymerization

DP was determined as method described by Klemm *et al*., (2005) and Karande *et al.,* (2011). The DP of both enset fiber cellulose (Ef-C) and Ef-MCC was determined by using cupper-ammonium hydroxide (Cuam) solution. Cuam is widely used for DP estimation by viscosity determination. The Cuam solution containing Cu and NH_3 is prepared by dissolving freshly precipitated Cu $(OH)_2$ in aqueous ammonia according to the following procedure. In 2 liters flask, 56 g of copper sulfate was dissolved in 1.2 liters distilled water and filtered into a beaker. By adding 28 ml of 25% aqueous ammonia, Cu $(OH)_2$ was precipitated. The precipitate was allowed to sediment, a clear supernatant solution was decanted and the precipitate was thoroughly washed with distilled water to remove sulfate ions. The moist sulfate-free Cu $(OH)_2$ was dissolved to 1000 ml of 25% ammonia solution at room temperature.

DP of Ef-C and Ef-MCC sample was measured by the viscosity method with the help of Ostwald capillary viscometer. To determine DP, 45 mg samples was dissolved in the 30 ml of Cuam solution. The mixture was vigorously shaken and then placed in water bath at 25 ^oC for 5 min. After the sample was completely dissolved in the solvent, appropriate volume of the solution was transferred to Ostwald capillary viscometer and viscosity measurement was carried out. DP was calculated from following equation.

$$DP = \frac{2000 * \eta spec}{c * (1 + 0.29 * \eta spec)} \quad \text{Eq. 3}$$

where, η_{spec}= specific viscosity; c is concentration in g/l, 0.29 is viscometer constant.

The specific viscosity was calculated from the efflux time, *t*, is the time required (in seconds) for the sample to travel from upper graduated mark to the lower graduated mark and $t_{0,}$ the time required for pure solvent to travel from upper graduated mark to the lower graduated mark.

$$\eta\text{spec} = \frac{\text{t}}{\text{to}} - 1 \quad \text{Eq. 4}$$

4.2.2.3. Fourier Transform Infrared spectroscopy (FTIR)

FT-IR analysis was conducted by using FTIR spectrometer (FTIR-8400S, SHIMADZU, Japan). Initially, the KBr disc was rinsed with alcohol. Then 8 mg of the sample was dissolved in liquid paraffin and coated with KBr. The KBr along with the sample was placed in KBr holder and eventually inserted into the FT-IR machine. Each IR spectrum was collected with 20 scans in the range of 4,000–400 cm^{-1} and spectral resolution of $8cm^{-1}$.

4.2.2.4. X-ray Diffraction (XRD)

The degree of crystallinity (*CrI*) of Ef-MCC powder prepared from enset fibers cellulose was determined using the X-ray diffractometer (XRD7000, SHIMADZU, Japan) using monochromatic CuKα radiation (λ= 1.5406 Å) at voltage of 40 kV and 30 mA power. Scattered radiation was detected in the range of 2θ= 10°-40° at a scan rate of 3º/min. The *CrI* was calculated using the following formula.

$$\text{C}_\text{r}\text{I} = \frac{\text{I}_{002} - \text{I}_{\text{am}}}{\text{I}_{002}} * 100 \quad \text{Eq. 5}$$

where I_{002} is the overall intensity of the peak at 2θ about 22º and I_{am} is the intensity of the baseline at 2θ about 18º respectively (Mihranyan *et al*., 2004).

The average crystallite size (L) of the direction perpendicular to 002 lattice planes was calculated as follows:

$$\text{L} = \frac{K\lambda}{\beta cos\theta} \quad \text{Eq. 6}$$

where K, the dimensionless constant of value 0.94; λ is the X-ray wavelength (0.1542 nm); β is the line broadening at half the maximum intensity; θ is the Bragg's angle corresponding to the 002 planes (Kambli *et al*., 2017).

4.2.2.5. Thermal analysis (TGA)

Thermal analysis was performed between temperature range of 20 ^{o}C and 700 ^{o}C in dry nitrogen with a flow rate of 50 ml/min in a thermogravimetric (TG)/differential thermal analysis (DTA) apparatus (DTG-60H, Japan). The weight percentage of residue was recorded to determine the weight losses of the sample after heating.

4.2.2.6. Scanning electron microscopy (SEM)

The SEM micrographs of Ef-C and Ef-MCC were analyzed by a scanning electron microscope (JOEL, JSM-IT300, Japan) at a voltage of 20kV and photomicrographs of the powders were taken.

4.2.3. Powder properties of microcrystalline cellulose

4.2.3.1. Moisture content

The moisture content (Mc) of cellulose and Ef-MCC was determined as follows; 3 g of sample was uniformly placed onto pre-dried and weighed Petri dish and then dried in an oven at 105 °C until a constant weight was obtained. The percentage of Mc was calculated using the following formula.

$$\mathrm{Mc} = \frac{A - B}{A} * 100 \quad \text{Eq. 7}$$

where A and B are initial weight of sample before drying and constant weight after drying in g, respectively.

4.2.3.2. Water soluble substances

Five grams of MCC powder was placed in beaker and mixed with 80 ml of distilled water. The mixture was shaken using shaker (Heidolph unimax 1010, Germany) for 10 min and filtered with filter paper into flask. The filtrate was then transferred into a pre-weighed beaker and

evaporated to dryness at 105 ^{o}C for 1 h and weighed. The amount of soluble substance was the difference between the weight of beaker along with residue and the weight of empty beaker.

4.2.3.3. Ether soluble substances

Ten grams of MCC powder was placed in column chromatography and 50 ml of peroxide free-ether was passed through the column. Then eluate was collected and evaporated to dryness in a previously dried and tared evaporating beaker with the aid of a hot plate at 105 ^{o}C for 30 min. After all the ether has evaporated, the dried residue was cooled and weighted. The difference between the weight of the residue and weight obtained from blank was used to determined ether soluble component.

4.2.3.4. Hydration capacity

Hydration capacity (HC) was determined according to the method described by Umeh *et al*., (2014). A 1.0 g of each sample was placed in four 15 ml plastic centrifuge tubes and 10 ml distilled water was added and then stoppered. The contents were shaken for 20 min with 5 min interval. The mixture was centrifuged using Beckman coulter (Allegra 64R, Centrifuge) at 2000 rotation per minute (rpm) for 15 min. The supernatant was carefully decanted and the sediment was weighed. The HC was calculated as follows.

$$\mathrm{HC} = \frac{\text{Weight of tube with sediment} - \text{Weight of empty tube}}{\text{Weight of dry sample}} \ldots\ldots\ldots\ldots\ldots\ldots\ldots\ldots\ldots\ldots \text{Eq. } 8$$

4.2.3.5. Moisture sorption capacity

Moisture sorption capacity was determined using the method outlined by Mihranyan *et al*., (2004). Prior to moisture sorption determination, the Ef-MCC powder sample was dried in oven for 4 h at 105 ^{o}C. 1 g of the dried sample was spread evenly on plastic plate (pre-weighed) and placed in desiccators containing distilled water (100% RH), saturated solution of NaCl and appropriate concentrations of NaOH, i.e., 24.66%, 31.58% and 40% of NaOH solutions to provide 60%, 40% and 20% RH, respectively and stored at 25 ^{o}C. Samples were equilibrated for four weeks. The weights after four weeks were determined and the moisture uptake of each sample was calculated as the weight difference of before and after equilibration in a given RH.

Water sorption capacities of the Ef-MCC were expressed as percent moisture sorbed. Results were expressed as a mean of three parallel determinations.

4.2.3.6. Ash value determination

The ash value was determined according to the following procedure. A crucible was cleaned and oven dried at 100 ^{o}C for 30 min. Then, the crucible was cooled in desiccator containing silica gel for 30 min; 3 g of Ef-MCC powder was placed onto the crucible (pre-weighed) and heated starting from low temperature till the smoking was ceased. The sample was then charred in furnace at 550 ^{o}C for 2 h, cooled in desiccator from 45-60 min and weighed. The ash value was determined as ratio of weight difference of the charred residue obtained after 2 h and empty crucible to the weight of sample.

4.2.3.7. pH determination

The pH of Ef-MCC was determined as follows; 5 g of Ef-MCC sample was suspended in 40 ml distilled water and shaken for 20 min. The mixture was allowed to settle down and the pH of the supernatant was determined using pH meter (JENWAY, 3505, UK).

4.2.3.8. Densities and related properties

To determine the bulk density each of Ef-MCC-od, Ef-MCC-mod and Ef-MCC-sd powder, 30 g of powder sample was placed in measuring cylinder and the volume occupied by the powder was recorded. Then the bulk density was calculated by dividing weight of sample by volume of the sample powder. Tapped densities of the powders was determined using tapped density tester (ERWEKA, Germany). The bulk in the cylinder was tapped using tapp densitometer to a constant volume and tapped volume was recorded. Tapped density was then calculated based on the ratio of weight to tapped volume.

Carr's Compressibility Index and Hausner ratio were calculated from the data of bulk density and tapped density using Eq. 9 & 10 respectively.

$$\text{Carr's index(CI)} = \frac{\text{tapped density} - \text{bulk density}}{\text{tapped density}} * 100 \ldots\ldots\ldots\ldots\ldots\ldots\ldots\ldots\ldots\ldots\ldots\ldots \text{Eq. 9}$$

$$\text{Hausner ratio(HR)} = \frac{\text{tapped density}}{\text{bulk density}} \ldots\ldots\ldots\ldots\ldots\ldots\ldots\ldots\ldots\ldots\ldots\ldots\ldots\ldots\ldots\ldots\ldots\ldots\ldots\ldots\ldots\ldots\ldots\ldots \text{Eq. } 10$$

4.2.3.9. True Density

True density D_t, of the each Ef-MCC-od, Ef-MCC-sd and Ef-MCC-sd powder was determined by liquid displacement method using xylene as immersion fluid according to the method described in Oyeniyi and Achor (2014) and Kambli *et al.,* (2017). A cleaned glass bottle was filled with xylene followed by wiping off all spilled over xylene and weighed. The same bottle was emptied and cleaned thoroughly and 2 g of Ef-MCC powder was added into the bottle. The bottle was then half filled with xylene and stirred with glass rod to release air bubbles. Finally, the bottle was completely filled with xylene and the weight of bottle was noted as (b). True density of MCC was calculated using the following equation.

$$\text{Dt} = \frac{\text{w}}{[(\text{a} + \text{w})] - \text{b}} * \text{Sg} \ldots\ldots\ldots\ldots\ldots\ldots\ldots\ldots\ldots\ldots\ldots\ldots\ldots\ldots\ldots\ldots\ldots\ldots\ldots\ldots\ldots\ldots\ldots\ldots\ldots\ldots\ldots\ldots\ldots\ldots \text{Eq. } 11$$

where *w* is the weight of powder, *Sg* is specific gravity of xylene, *a* is weight of bottle + xylene and *b* is weight of bottle + xylene + powder.

4.2.3.10. Particle size analysis

Particle sizes were determined by laser diffraction particle-size analyzer (Mastersizer 2000, Malvern Instruments Ltd, Worcestershire, WR14 1XZ, UK). A small amount of Ef-MCC was dispersed in distilled water to provide an obscurity between 0.15-0.20. Determinations were done in triplicates. The analysis was done under these conditions: Range (0.05–900 µm, 300RF); active beam length (2.4 mm); sample unit (MS1: Small Volume Sample Dispersion Unit); Polydisperse; standard-wet, Presentation (3OHD).

4.2.3.11. Compressibility of microcrystalline cellulose

To study the compression property of Ef-MCC plain tablets, Ef-MCC powder and Avicel PH101 powders were compressed. Tablets were made using tablet compression machine (Eco Press200, India) using 50N, 75N, 100N, 125N and 150N compression forces. The desired compression force was adjusted indirectly using crushing strength of tablets formulated by Avicel PH101.

Because of poor flow properties, the powder was manually filled into the die with the target weight of 400 mg.

4.2.4. Evaluation of microcrystalline cellulose tablets

The batches of the compacts were each allowed a 24 h post compression relaxation time before evaluation for crushing strength, tensile strengths, friability and disintegration time.

4.2.4.1. Diametrical crushing strength test

A tablet was placed radially between the jaws of a tablet hardness tester (CALEVA, UK) and the force needed to disrupt the tablet by crushing was determined. A total of 10 tablets were evaluated from each batch and the results were given as the mean values of these measurements. The mean and standard deviation were determined.

4.2.4.2. Tensile strength

The tensile strengths (TS) of the compacts were determined based on the crushing strength, thickness and tablet diameter using Eq. 12.

$$TS = \frac{2F}{\pi DT} \quad \text{Eq. 12}$$

Where F is the breaking force, D is the tablet diameter, T is the tablet thickness.

4.2.4.3. Friability test

Ten tablets randomly selected from each batch of the compacts and collectively weighed. Then, the tablets were placed in a friability tester (ERWEKA, TAR 20, Germany) and the friabilator programmed to revolve at 25 revolutions per min (rpm) for 4 min. At the end, the tablets were collected and dedusted. The tablets were reweighed and the abrasion resistance (B) calculated from Eq. 13.

$$B\ (\%) = 1 - \frac{w}{w_o} \quad \text{Eq. 13}$$

where w_o is the initial weight and w is the final weight.

4.2.4.4. Disintegration time test

Six tablets randomly selected from each batch were used for the test. The test was carried out using a disintegration test apparatus (Erweka, Germany) and each compact held in place with a glass disc inside each cylindrical hole. Each beaker was filled with 900 mL of distilled water heated to a temperature of 37 ± 1 °C. The time taken for each compact to completely break up and pass through the mesh was noted.

4.2.5. Lubricant sensitivity of Enset fiber microcrystalline cellulose

To evaluate lubricant sensitivity, tablets containing Ef-MCC-sd, Ef-MCC and Avicel PH101 were compressed with and without fixed concentration of magnesium stearate at fixed compression force.

The lubricant sensitivity was expressed as the lubricant sensitivity ratio (LSR) (Medina and Kumar, 2007).

$$LSR = \frac{S_o - S_{lub}}{S_o} \quad \text{Eq. 14}$$

Where, So is compact crushing strength without lubricant, and S_{lub} is compact crushing strength with added lubricant.

4.2.6. Drug-Microcrystalline cellulose compatibility studies

The compatibility study of paracetamol and Ef-MCC (physical mixture at 1:1 ratio) was carried out using Fourier Transform Infrared Spectrophotometer (FTIR 8400-S, SHIMADZU, Japan) as per method described in section 2.2.2.4.

4.2.7. Preparation of tablets for dilution potential study

To study dilution potential of different samples of Ef-MCCs tablets were prepared by incorporating paracetamol at concentrations of 35%, 50%, 65% and 80% w/w on the basis of evidences literatures (Habib *et al*., 1996; Kuentz and Leuenberger, 2000) in 400 mg. Specified amount of each Ef-MCCs and Avicel PH101 was mixed with paracetamol in a Turbula® mixer (Willy A. Bachofen AG, Maschinefabrik, Basel, Switzerland) for 5 min. Paracetamol tablets

were prepared by using tablet compression machine (Eco Press200, India) at a constant compression force (adjusted to achieve > 40N crushing strength for the standard Avicel PH101 using flat punches of diameter 11 mm. The results were compared with dilution potential of Avicel PH101 tablets prepared at aforementioned concentration and crushing strength.

4.2.8. Construction of calibration curve of paracetamol

A stock solution containing 200 µg/ml of paracetamol in phosphate buffer of pH 5.8 was prepared. Different volumes of stock the solutions were taken and then diluted to provide seven different concentrations (3.5, 5.5, 7.5, 9.5, 11.5, 13.5 and 15.5 µg/ml) of paracetamol in phosphate buffer. The UV absorbance readings of these solutions were measured at 243 ηm using UV/Visible spectrophotometer (UV/VIS Spectrophotometer, T92+, PG instruments limited). Phosphate buffer (pH 5.8) was used as a blank.

4.2.9. Invitro Drug Release Study

The dissolution test was done according to the USP specification using dissolution apparatus Type II (ERWEKA, DT600, Germany) with 900 ml phosphate buffer (pH 5.8) as the dissolution medium at 37 ± 0.5 ºC and 50 rpm. 5 ml aliquots of the dissolution medium were removed at 5, 10, 15, 20, 30, 45 and 60 min and filtered using filter paper. Equal amount of fresh medium kept at the same temperature was transferred into the dissolution vessel to keep a sink condition. 1 ml of the filtered samples was diluted to 25 ml and absorbance readings were taken with UV/Visible spectrophotometer (UV/VIS Spectrophotometer, T92+, PG instruments limited) at 243 ηm. Phosphate buffer (pH 5.8) was used as a blank.

4.2.10. Statistical Analysis

The results were analyzed using Analysis of Variance (ANOVA) with a statistical software Origin 2019 (OriginLab™ Corporation, USA). Tukey multiple comparison test was used to compare the individual difference in the physicochemical and tablet properties of the MCC. At 95% confidence level, p values less than or equal to 0.05 were considered statistically significant.

5. RESULTS AND DISCUSSION

5.1. Isolated Enset Fiber Cellulose and Microcrystalline Cellulose

The present study dealt with extraction and characterization of cellulose from enset fiber, preparation of Ef-MCCs and its evaluation as directly compressible excipient. Cellulose was extracted from enset fiber using formic acid/acetic acid. From the result of preliminary study, acid/acetic acid gave Ef-C with better organoleptic properties compared to Ef-C extracted by other extraction methods such as hot water and formic acid pretreatment. Organoleptically, the enset fiber cellulose obtained was white, fluffy and fibrous material (Figure 4 a). Ef-MCCs were prepared by acid hydrolysis and the resulting Ef-MCC powders were odorless, tasteless and physically appeared as fine powder as illustrated in Figure 4 b.

(a) (b)

Figure 4: Ef-C (a) and Ef-MCC (b).

5.2. Yield of Cellulose and Microcrystalline Cellulose

The yield of each of Ef-C and Ef-MCC was determined as an average of three batches on dry basis. The percent yield of Ef-C, Ef-MCC-od, Ef-MCC-mod and Ef-MCC-sd are given in Table 1. The results indicate that enset fiber is promising potential source of cellulose and MCC. The yield of Ef-MCC-mod significantly higher than Ef-MCC-od. Microcrystals are tightly packed in native cellulose. The interconnected microcrystals do not disintegrate by acid hydrolysis alone and freed by mechanical disintegration (Battista and Smith, 1962). The

increased yield of Ef-MCC-mod might be attributed to mechanical agitation. On the other hand, lower yield of Ef-MCC-sd, anticipated to the large size of the spray drier equipment which affect the recovery of powder.

Table 1: Percent yield of Ef-C and Ef-MCC products.

Samples		Yield (%)
Ef-C		56.97 ± 1.3
Ef-MCCs	Ef-MCC-od	72.8 ± 1.02
	Ef-MCC-mod	82 ± 1.6
	Ef-MCC-sd	65.42*

Mean ± SD, * indicates single determination

5.3. Physicochemical characterization

5.3.1. Identification Test

As it was observed from the experimental result of identification test, the color of both extracted cellulose and Ef-MCC were turned to violet-blue in iodinated zinc chloride solution. The presence of violet-blue color is indicative of cellulose/MCC which is in agreement with USP 30/NF 25 specification.

5.3.2. Degree of Polymerization

DP helps to understand the number of repeating units in polymer and it is used as an identity test, as pharmacopeial MCC is defined by a DP below 350 glucose units (Kambli *et al*., 2017). The DP value of Ef-MCC-od, Ef-MCC-sd and Ef-MCC-mod was found to be 315.12, 311.5 and 309.03, respectively. These values are less than 350 that is typical characteristic of MCC. The molecular weight, which is dependent on the number of polymer chains, was calculated from DP by multiplying the value of DP with molecular weight of glucose, i.e., 162 (Shanmugam *et al*. 2015). Accordingly, the molecular weight of Ef-MCC-od, Ef-MCC-sd and Ef-MCC-mod was 51049.44 g/mol, 50463 g/mol and 50062.86 g/mol, respectively. Avicel PH101 has DP of 225.08 and molecular weight of 36462.96 g/mol. On the other hand, the DP of Ef-C was found to be 567 with corresponding molecular weight of 92016 g/mol.

5.3.3. Fourier Transform Infrared Spectra Analysis

FT-IR spectrum for Ef-C, Ef-MCC and Avicel PH101 are presented in Figure 5, Figure 6 and Figure 7, respectively.

Peaks occurred at 3355 cm $^{-1}$ in native enset fiber cellulose were assigned to hydroxyl (-OH) group stretching vibrations. These absorption bands appeared at 3188 cm^{-1} for Avicel PH101. According to Duan *et al*. (2017) and Krstic *et al*., (2018), a broad absorption band observed at 3100-3700 cm^{-1} in the FTIR spectra indicates the presence of -OH stretching vibrations of cellulose when the chemical structure of MCC is analyzed. The peak at 2923-2852 cm^{-1} is attributed to C-H stretching vibration in cellulose or MCC so does for Avicel PH101(Duan *et al*., 2017).

The bands around 1460 cm $^{-1}$ were attributed to the asymmetric –CH_2 bending (Zhang *et al.*, 2013; Elanthikkal *et al*., 2010; Krstic *et al*., 2018). These absorption bands occurred around 1460 cm $^{-1}$ in all extracted Ef-C, Ef-MCC and Avicel PH101. The peak round 1377 cm $^{-1}$ represent O-H bending (Sun *et al*., 2004). The absorbance around 1313 cm^{-1} arises from the -CH asymmetric bending and C-C skeletal stretching vibrations (Sun *et al*., 2004; Elanthikkal *et al*., 2010).

The peak associated to –C–O–C– stretching of the β-1,4-glycosidic linkage was observed around 1160 cm^{-1} for all the samples (Sun *et al*., 2004; Haafiz *et al*., 2013; Krstic *et al*., 2018). The peak around 1110 cm^{-1} belongs to C-OH skeletal stretching vibration (Liu *et al*., 2006; Morán *et al*., 2008). The absorption band around 1041 cm^{-1} representing C-O-C stretching vibration in pyranose ring. This absorption is consistent with those of the typical cellulose backbone (Elanthikkal *et al*., 2010; Haafiz *et al*., 2013; Setu *et al*., 2014). Additionally, the peak in the broad band of 925-840 cm^{-1} attributed to the typical structure of cellulose due to the β-glycosidic linkages of the glucose ring of cellulose chain and is attributed to the -C_1-H bending with ring vibration contribution (Liu *et al*., 2006; Elanthikkal *et al*., 2010).

Despite some small differences, the FT-IR spectra of the Ef-C, Ef-MCC and Avicel PH101 samples exhibit all the characteristics of cellulose. Over all, the peaks present around 1461, 1377, 1313, 1158, 1041 and 925-840 cm^{-1} represent typical cellulose absorption peaks (Chieng

et al., 2017). And all spectral results revealed that Ef-C and Ef-MCCs have similar typical absorption band characteristics to Avicel PH101 which indicate that, the prepared Ef-C and Ef-MCC have similar characteristics and chemical composition to Avicel PH101.

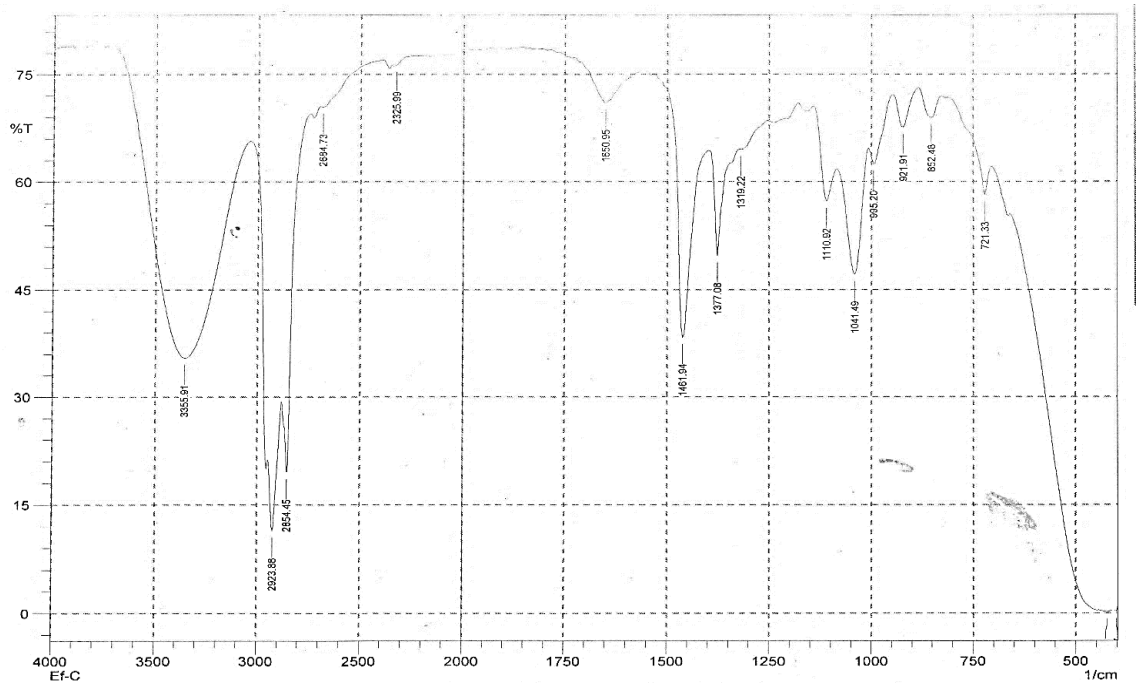

Figure 5: FTIR spectrum of Ef-C.

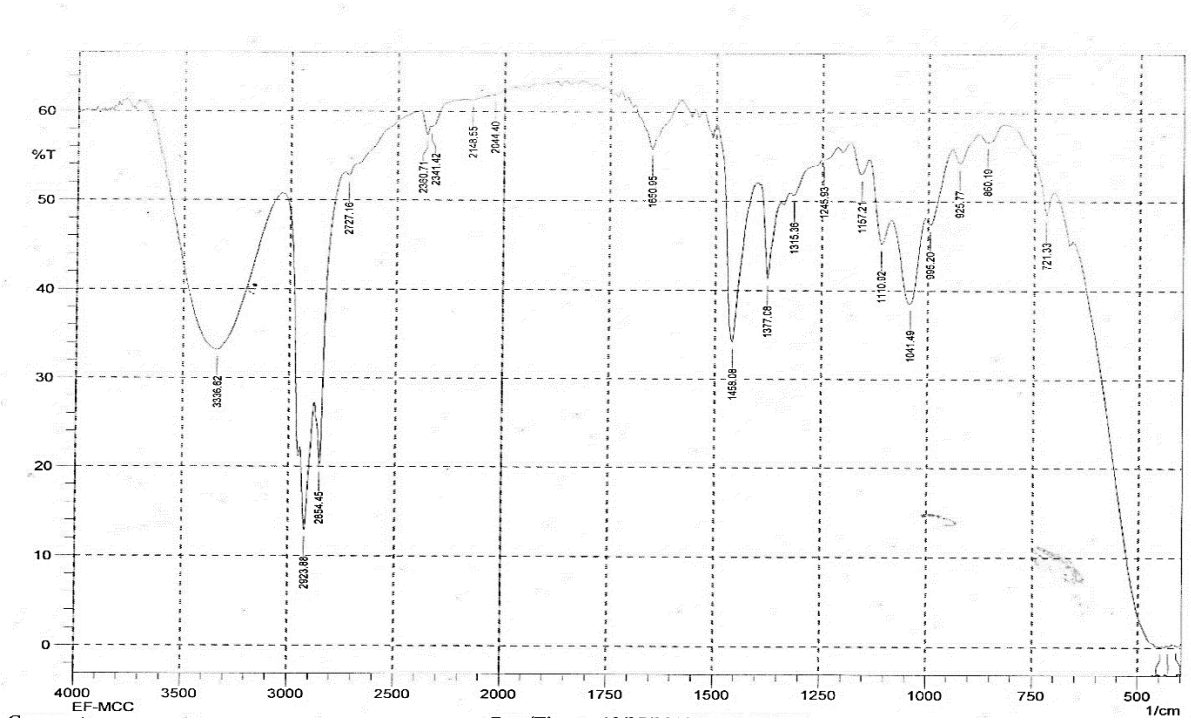

Figure 6: FTIR spectrum of Ef-MCC.

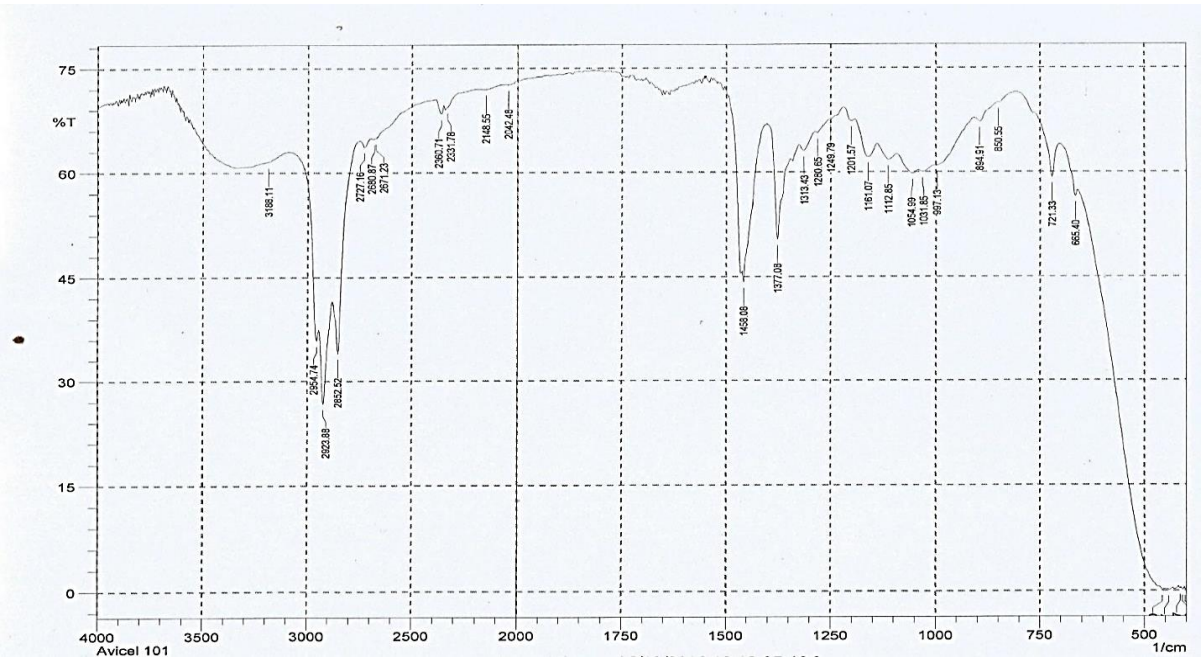

Figure 7: FTIR spectrum of Avicel PH101.

5.3.4. X-ray Diffraction Analysis

The degree of crystallinity influences various properties including the compactibility and the adsorption of water. These could influence the flowability and the drug stability. In the region of amorphous cellulose, a fraction of adsorbed water can be bound strongly, e.g., by hydrogen bonding to hydroxyl groups in each repeating sugar unit in the cellulose (Podczeck and Révész, 1993). In order to analyze the crystallinity of Ef-C and Ef-MCC powders obtained in this work, XRD was carried out and the crystallinity index (%CrI) value was computed to quantify the crystallinity of the samples. The XRD patterns of Ef-C, prepared MCC and Avicel PH101 are illustrated in Figure 8 (a-f). The peak positions of I_{002} and I_{am} at $2\theta = 22^{o}$ and $2\theta = 18^{o}$ respectively, are typical for type Iβ cellulose (Deraman *et al*., 2001). Thus, Ef-C and Ef-MCC were present in the form of cellulose Iβ and not cellulose II, which arises from the fact that there is no doublet in the intensity of the main peak and it is obtained from higher plant (Morán *et al*., 2008).

The peak at $2\theta = 22.48^{o}$ for Ef-MCC-od, $2\theta = 22.54^{o}$ for Ef-MCC-sd and $2\theta = 22.66^{o}$ for Avicel PH101 was sharper and the sharper diffraction peak is an indication of higher crystallinity index (Alemdar and Sain, 2008).

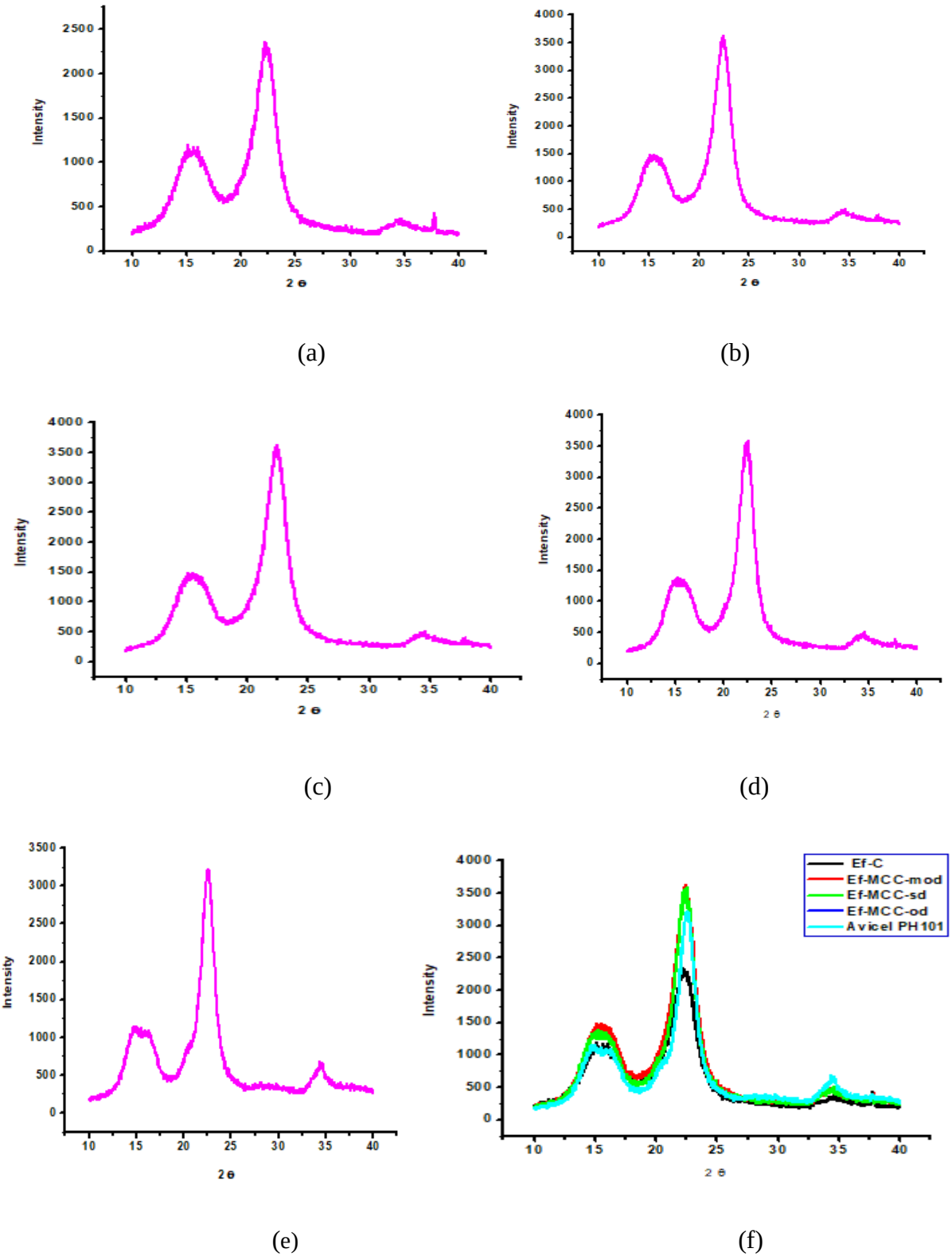

Figure 8: XRD of Ef-C (a), Ef-MCC-od (b), Ef-MCC-mod (c), Ef-MCC-sd (d), Avicel PH101 (e) and superimposed (f).

The CrI was calculated for each Ef-C, Ef-MCC-od, Ef-MCC-mod, Ef-MCC-sd and Avicel PH101. The calculated crystallinity index and crystallite size of the different MCC samples are given in Table 2. The %CrI of the Ef-MCC products varied from 85% to 89%. Ef-C has lower %CrI than its Ef-MCCs counterpart. This might indicate that acid hydrolysis effectively removed amorphous region of Ef-C and resulted in increased crystallinity of Ef-MCCs.

Table 2: Crystallinity index and crystallite size of Ef-MCC samples and Avicel PH101.

Samples	Peak intensity (at I_{am})	Peak intensity (at I_{002})	%CrI	L(nm)
Ef-C	498	2316	78.5	3.02
Ef-MCC-od	340	3254	89.57	4.05
Ef-MCC-mod	443	3073	85.57	3.24
Ef-MCC-sd	432	3522	87.73	3.60
Avicel PH101	327	3141	89.59	4.047

CrI- Crystallinity index, L- crystallite size

The value of CrI of Ef-MCC-od and Ef-MCC-sd are almost similar to the CrI value of Avicel PH101 as can be noticed from Table 2. This also evidenced by superimposed diffractograph as depicted in Figure 8 (f) above. However, CrI of Ef-MCC-mod was slightly lower than the value for Avicel PH101. The Decrease in crystallinity of Ef-MCC-mod might be due to mechanical effect of agitation and pulverization because grinding reduces the crystallinity of material as reported elsewhere (Suzuki and Nakagami, 1999; Kumar *et al*., 2009). Study by Suzuki and Nakagami, (1999) revealed that degree of crystallinity of MCC powders was reduced from 65% to 12.1% through grinding in a vibratory mill. On the other hand, the crystallinity increased with decreased DP (Iida *et al*, 1997) and increased crystallite sizes, because the crystallites surface corresponding to amorphous cellulose regions diminished (Poletto *et al.*,2014). In general, MCC is typically characterized by a high degree of crystallinity, although there are variations between values (Chuayjuljit *et al*., 2010). This is because, cellulose obtained from different origins and hydrolysis conditions differ in crystallinity (De Menezes *et al.*, 2009) and hence resulting in difference in MCC crystallinity.

5.3.5. Thermogravimetric and Differential Thermal Analysis

Figure 9 illustrates the TGA of enset fiber, Ef-C, Ef-MCC and Avicel PH101. As can be seen in the Figure 9, during the increase of temperature, the decrease in the weight of the sample took place. The decomposition of untreated (raw) enset fiber (Ef-R), Ef-C, Ef-MCC and Avicel PH101 started at 39, 51, 50 ^{o}C and 56 ^{o}C, respectively and a rapid weight loss occurred in the temperature range of 193-370 ^{o}C, 217- 350 ^{o}C, 318-360 ^{o}C and 311-370 ^{o}C, respectively.

Ef-R TGA curve showed an initial weight loss between the temperature range of 39–101 ^{o}C which corresponds to a weight loss of 6.01%. Similarly, the first stage weight loss was observed in the temperature range of 51-101^{o}C, 50-101^{o}C and 56-108 ^{o}C for Ef-C, Ef-MCC and Avicel PH101, respectively, with corresponding weight loss of 4.16%, 4.64% and 5.81%. The weight loss in the region of 50-100 ^{o}C is mainly due to moisture evaporation (Deepa *et al*., 2015).

The second and major decomposition peak was observed at about 193-370 ^{o}C, 217-350 ^{o}C, 318-360 ^{o}C and 311-370 ^{o}C for Ef-R, Ef-C, Ef-MCC and Avicel PH101, respectively. According to literature evidence, this temperature range could be attributed to the decomposition behaviors of the major constituents of the natural fiber: cellulose, hemicellulose, lignin and ash. Since hemicelluloses and cellulose components are degraded first, they are the main contributors to the evolution of the volatile compounds while lignin is degraded later and mainly responsible for the char portion of the product (Adel *et al*., 2011).

In Ef-R TGA curve, the decomposition peak appeared at about 193-370 ^{o}C which resulted in weight loss of 63%. This is attributed to thermal depolymerization of hemicelluloses and cleavage of glycosidic linkages of cellulose as reported by Ouajai and Shanks (2005). As can be noticed from the curve, the thermal decomposition of Ef-R started at low temperature as compared to Ef-C. It can be anticipated that the presence of hemicellulose constituents which decompose at low temperatures cause early onset of degradation (Mandal and Chakrabarty, 2011). The degradation in the wide temperature range of 200-500 ^{o}C corresponds to lignin (Carrier *et al*., 2010). The reason is that, lignin is full of aromatic rings with various branches. The activity of the chemical bonds in lignin covered an extremely wide range which led to the degradation of lignin occurring in a wide temperature range (Ouajai and Shanks, 2005; Yang *et al*., 2007). For Ef-C, within a wide range near 217-350 ^{o}C, 71.40% of weight loss was observed.

This is suggested to degradation processes of cellulose such as depolymerization and decomposition of glycosyl units followed by the formation of a charred residue according to Oliveira *et al*., (2011) and Trache *et al.*, (2014). The same event is observed in Ef-MCC and Avicel PH101 in temperature range of 318-367 ºC and 311-370 ºC respectively, with corresponding weight loss of 72.20% and 70.5%. Ef-C, Ef-MCC and Avicel PH101 have almost the same decomposition temperatures in the range of 250–350 ºC. On the other hand, TGA curve of Ef-MCC and Avicel PH101 revealed an increment in decomposition temperatures compared to Ef-C and hence increased thermal stability. This behavior suggests that celluloses with higher crystallinity and crystalline size exhibit higher thermal stability (Kim *et al*., 2010; Maiti *et al.*, 2013; Poletto *et al.*, 2011). Therefore, the higher thermal stability of Ef-MCC well agrees with its higher crystallinity and crystalline size as compared to Ef-C.

The thermal decomposition process was completed by a third step occurring at temperature range of 370-697ºC, 350- 690 ºC, 360- 697 ºC and 370-700 ºC for Ef-R, Ef-C, Ef-MCC and Avicel PH101, respectively. This temperature range resulted a smaller estimated mass loss of 12.5%, 11.17%, 11.97% and 14.59% for Ef-R, Ef-C, Ef-MCC and Avicel PH101, respectively.

The mass loss above 420 ºC may be due to oxidative degradation of the charred residue (Ouajai and Shanks, 2005) and the charring process was highly exothermal (Yang *et al*., 2007).

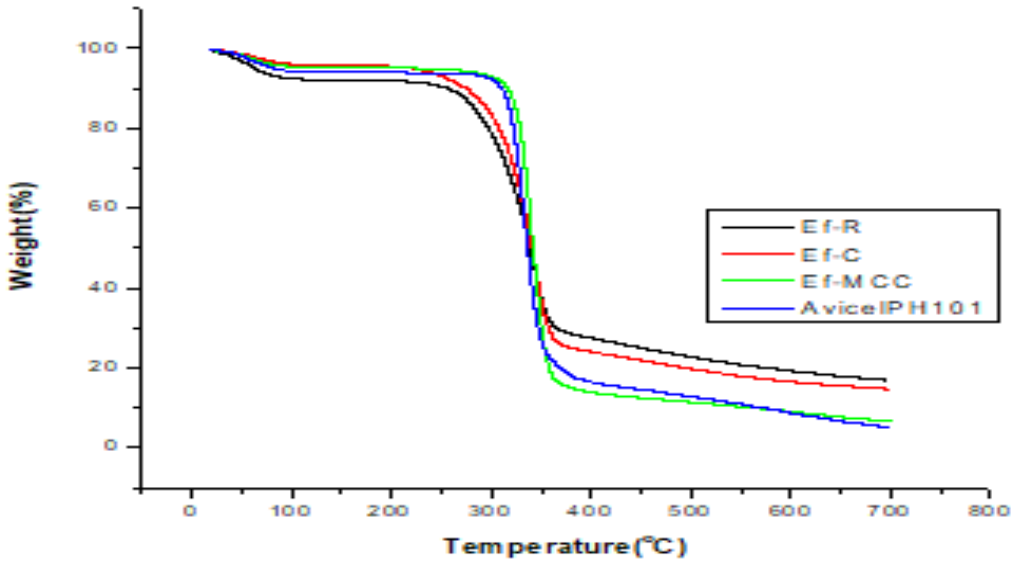

Figure 9: TGA curve of untreated enset fiber, Ef-C, Ef-MCC and Avicel PH101.

The DTA curves (Figure 10) also showed a characteristic change in the thermal decomposition. A small endothermic peak of Ef-R, Ef-C, Ef-MCC and Avicel PH101 appeared in the temperature range corresponding to evaporation of water i.e. at 61ºC, 69 ºC, 64ºC and 63 ºC, respectively. Such type of moisture loss is also corroborated by the TGA studies. Ef-MCC and Avicel PH101 revealed the second endothermic peak at 344 ºC and 333 ºC, respectively. The large endothermic peak appeared in this temperature range consistent with the rapid weight loss from TGA curve. The second endotherm in each case is an indication of the course of fusion or melting which gives an idea of the nature of decomposition of the crystallites (Mandal and Chakrabarty, 2011).

As can be noticed from the TGA and DTA curves, as purity of samples increased from Ef-R to Ef-MCC, the thermal stability improved as well. Moreover, the Ef-C and Ef-MCC should not be heated above 217 ºC and 318 ºC, respectively as heating above these temperate lead to heat decomposition while heat stable below the specified temperatures.

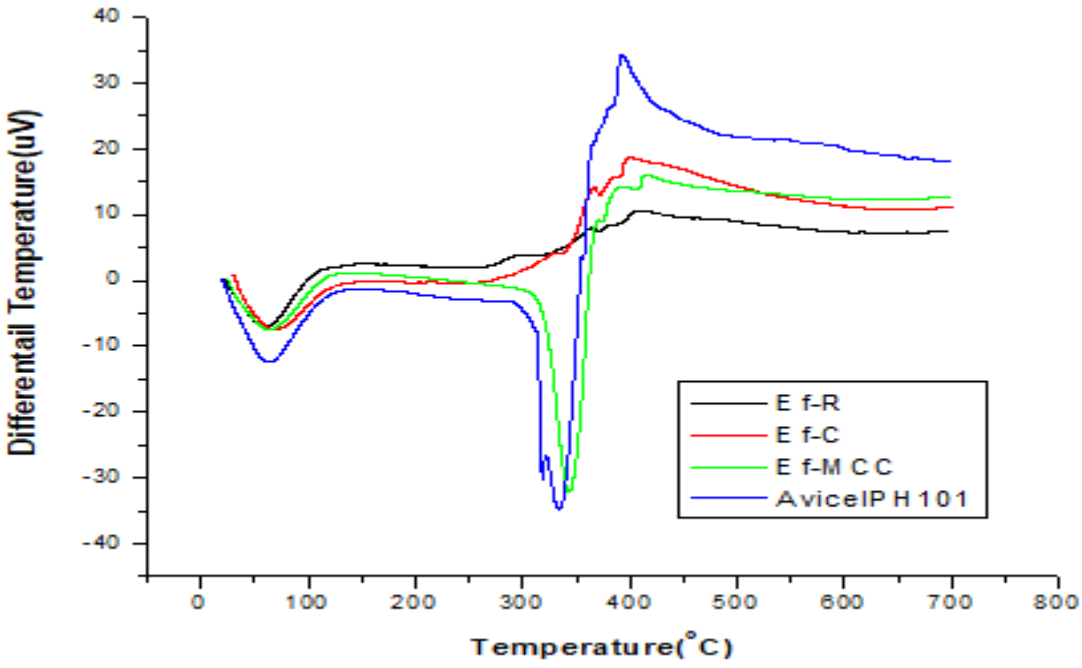

Figure 10: DTA curve of untreated enset fiber, Ef-C, Ef-MCC and Avicel PH101.

5.3.6. Morphological Characteristics

SEM was used to examine the surface morphology of the Ef-C and Ef-MCC-sd. The SEM micrographs (at different magnifications) for Ef-C and Ef-MCC are presented in Figure 11 and Figure 12, respectively. SEM micrographs showed changes in the morphology of the Ef-C in terms of shape, size and level of smoothness after acid hydrolysis. Accordingly, Ef-MCC-sd exhibited little aggregates of particles, rod-shaped, rough surface and shorter fibers strands. The shorter fiber strands of Ef-MCC-sd might be due to hydrolysis of Ef-C with hydrochloric acid which affects Ef-C morphology (Alemdar and Sain, 2008). The higher magnifications also revealed that the surface structure of the Ef-MCC-sd particles to be porous. The porous nature might be attributed to spray drying as spray drying creates porous particles. Whereas Ef-C exhibited a smooth fiber surface and a ribbon like structure with some network-structure.

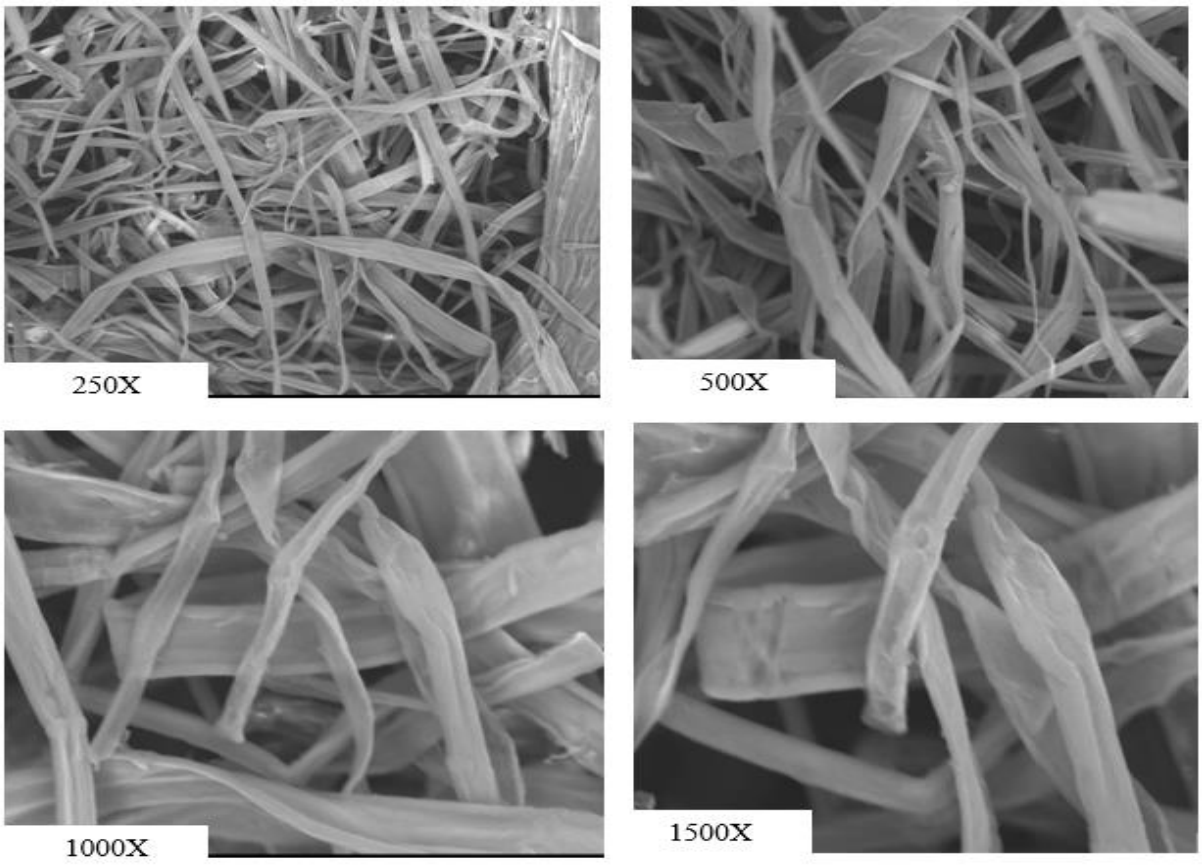

Figure 11: Scanning electron micrographs of Ef-C at different magnifications.

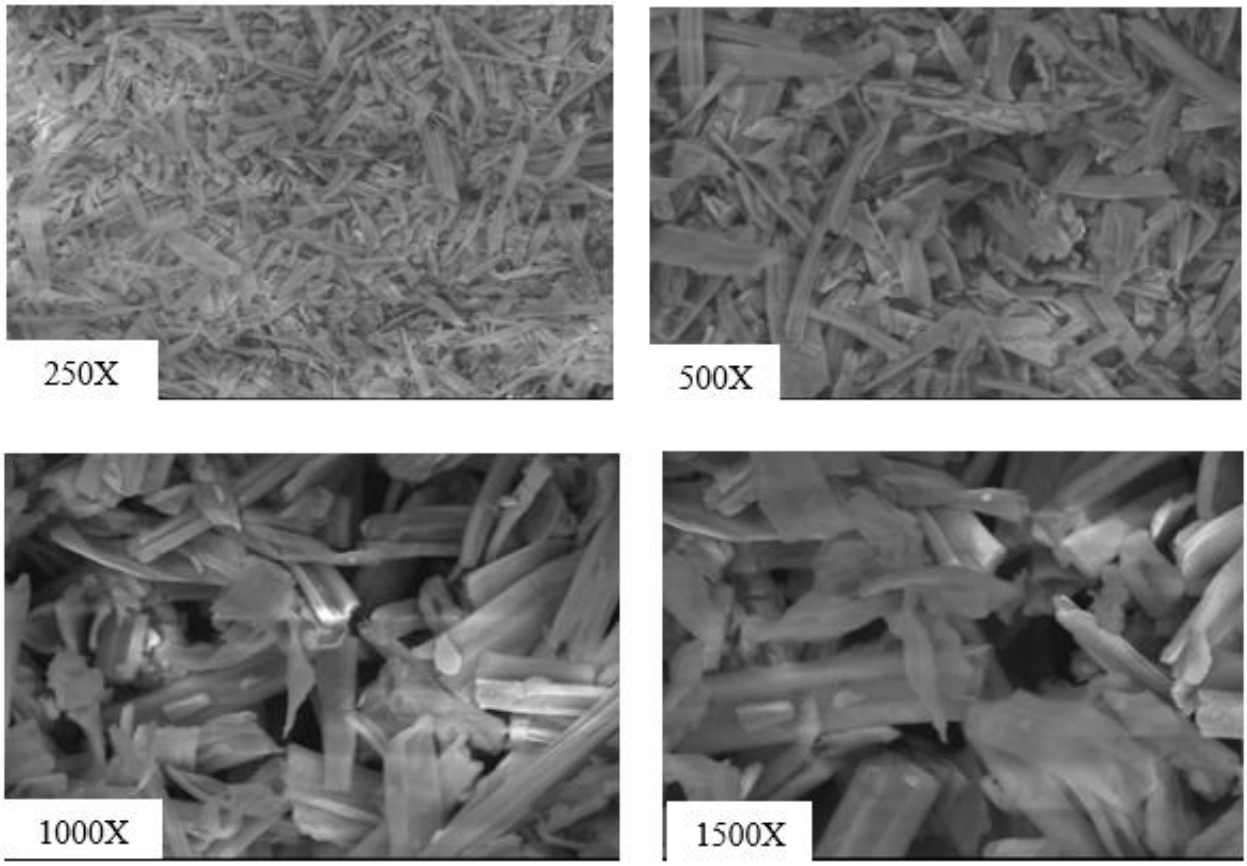

Figure 12: Scanning electron micrographs of Ef-MCC-sd at different magnifications.

5.4. Powder properties of microcrystalline cellulose

5.4.1. Moisture contents

Moisture content was expressed as weight loss on drying. As given in Table 3, the moisture contents of Ef-MCC products are comparable to Avicel PH101 ($p>0.05$). Moisture content for each sample was found to be less than 7% w/w which is the upper limits of USP (USP 30/NF 25, 2007). Many of MCC tableting properties depend on its moisture content. Moreover, moisture content of MCC has also been reported to cause stability problems for moisture sensitive drugs. Moisture content is often coupled with increased cohesiveness, chiefly because of interparticle liquid bridge formation (Mihranyan *et al*., 2004). Beside these, moisture is among all factors affecting a product's storage as it strongly influences microbial growth (Ganesan *et al*, 2008). Thus, lower moisture contents are required for safe storage as higher moisture contents can lead to microbial damage and subsequent deterioration in quality.

Several investigators have observed a direct relationship between moisture content and degree of crystallinity. In general, lower degree of crystallinity higher moisture content. This is because the lower the degree of crystallinity, the larger the number of free hydroxyl groups available for interaction with water molecules. The variability seen in the moisture content values among the various low or high crystallinity cellulose products, however, suggest that not only the degree of crystallinity, but also the accessibility of the adsorption sites to water molecules, determines the final moisture content (Kothari *et al*., 2002).

5.4.2. Hydration capacity

Hydration capacity has been described as the amount of water a material is able to absorb on hydration (Nkemakolam and Ifeanyi, 2017). Ef-MCC-od and Avicel PH101 had significantly higher hydration capacity compared to Ef-MCC-mod and Ef-MCC-sd (Table 3). This difference might be due to initial moisture content. Initial moisture content is among the other factors that govern hydration capacity. Powder with lower initial moisture content has relatively higher affinity to absorb water from the environment (Nkemakolam and Ifeanyi, 2017).

Table 3: Moisture content and hydration capacities of Ef-MCC-od, Ef-MCC-mod, Ef-MCC-sd and Avicel PH101.

Powder properties	Ef-MCC-od	Ef-MCC-mod	Ef-MCC-sd	Avicel PH101
Moisture content (%)	4.98 ± 0.33	5.31 ± 0.001	5.27 ± 0.23	5.10 ± 0.16
Hydration capacity	2.3 ± 0.04	1.72 ± 0.01	1.49 ± 0.08	2.10 ± 0.01

Mean ± SD (n=3)

5.4.3. Moisture sorption pattern

Knowledge of moisture sorption profiles is necessary where powder flow or compaction is critical (Gebre-Mariam and Schmidt, 1996a). The experimentally measured moisture sorption isotherms of Ef-MCCs and Avicel PH101, equilibrated at various relative humidity (RH) (20, 40, 60, 75.6 and 100%) for four weeks are depicted in Figure 13. The moisture sorption studies revealed that water uptake increased with increased relative humidity (RH). The moisture uptake

of Ef-MCC-mod is significantly higher than that of Avicel PH101 ($p<0.05$). However, there is no statistically significant variation between Ef-MCC-od, Ef-MCC-sd and Avicel PH101. The moisture sorption of the MCC is related to the crystallinity of the powders and the low values of moisture uptake are indicative of higher crystallinity (Bhimte and Tayade, 2007; Wang *etal*., 2010). The difference seen in the moisture sorption behavior may be attributed to difference in crystallinity of Ef-MCC-mod and Avicel PH101. Therefore, Ef-MCC-mod require more moisture control as it is more sensitive to environmental humidity.

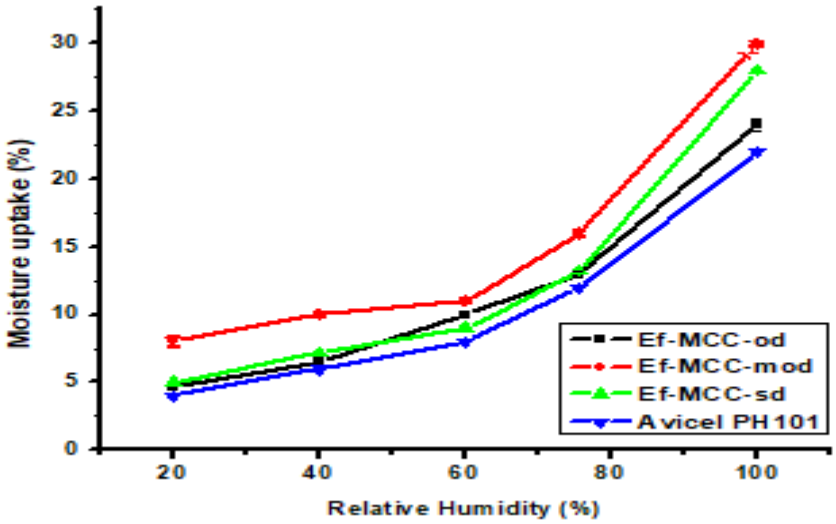

Figure 13: Moisture sorption patterns of Ef-MCC products and Avicel PH101.

5.4.4. Ash value

Ash value is the amount of residual substance which is not volatilized from a sample when the sample is ignited. The test is usually used for determining the content of inorganic impurities in an organic substance. The ash content of Ef-MCC-sd powder and Avicel PH101 were found to be 0.03% and 0.06, respectively. These values are in agreement with USP specification (Table 4). The low percentage of ash in the product may be as a result of very low inorganic materials usually present in cellulosic materials.

5.4.5. pH

The pH value of suspension of Ef-MCC-sd in water are given in Table 4. This pH value is within USP limit (USP 30/NF 25, 2007). Knowledge of the pH of an excipient is an important parameter in determining its suitability in formulations since the stability and physiological activity of most preparations depends on pH. The pH of Ef-MCC-sd was near neutral as shown by the pH values obtained. This quality is suitable for the formulation of both acidic and basic drugs (Nkemakolam and Ifeanyi, 2017).

5.4.6. Water and ether soluble substances

Water and ether soluble substances of Ef-MCC-sd and Avicel PH101 were within allowable limits (Table 4). However, the value of ether soluble substances of Ef-MCC-sd was significantly higher than that of Avicel PH101. This might be attributed to nature of the source material.

Table 4: Ash value, pH, water and ether soluble substances of Ef-MCC-sd and Avicel PH101.

Tests	Ef-MCC-sd	Avicel PH101	USP specification
Water soluble substance (%)	0.17 ± 0.01	0.21 ± 0.05	≤ 0.25
Ether soluble substance (%)	0.046 ± 0.003	0.025 ± 0.006	≤ 0.05
Ash value (%)	0.03 *	0.06*	≤ 0.1
pH	6.76 ± 0.04	6.3 ± 0.1	5.0 to 7.5

Mean ±SD (n=3), * indicates single determination

5.4.7. Powder Particle Size and Specific Surface Area

Particle size and specific surface area may be considered among the most important powders attributes. This is because particle size and specific surface area affect the flow and tableting properties of powders. It may impact tablet hardness, friability, disintegration and content uniformity (Kushner, 2013; Thoorens *et al*., 2014). The particle size analysis of each Ef-MCC-od, Ef-MCC-mod and Ef-MCC-sd samples was carried out to determine the particle size and size distribution (Figure 14 to Figure 17).

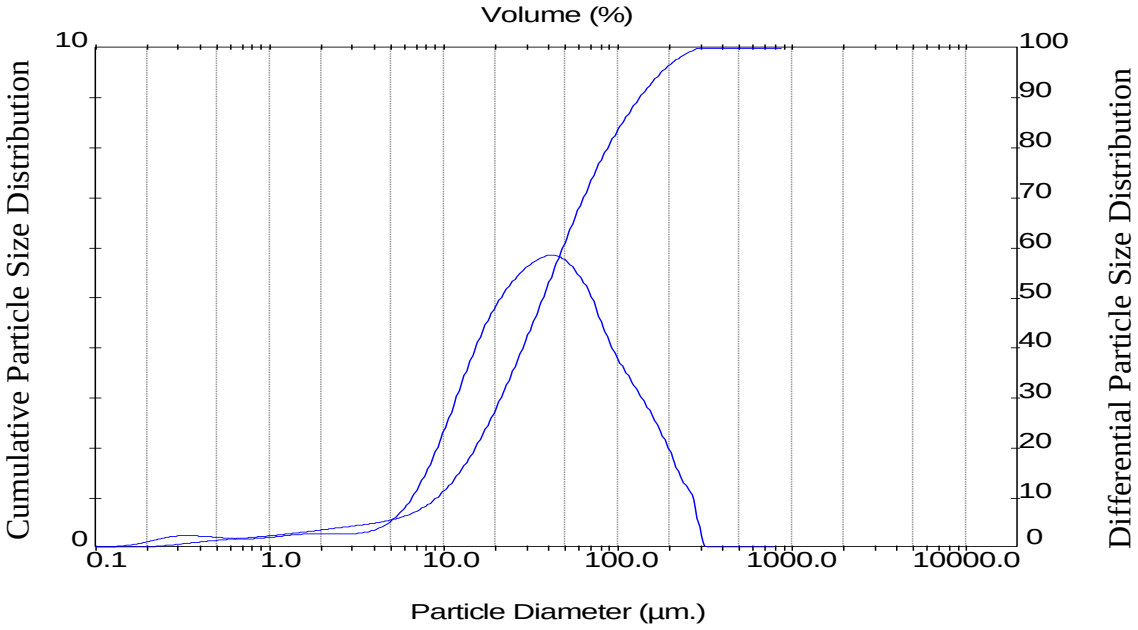

Figure 14: Volumetric particle size distributions of Ef-MCC-od.

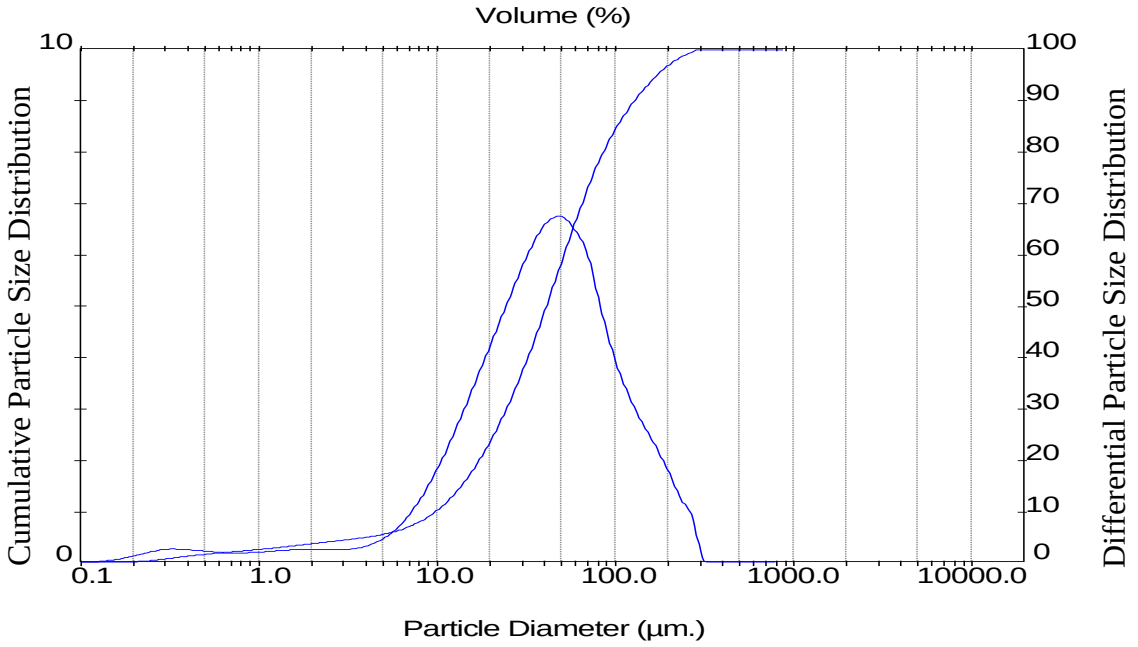

Figure 15: Volumetric particle size distributions of Ef-MCC-mod.

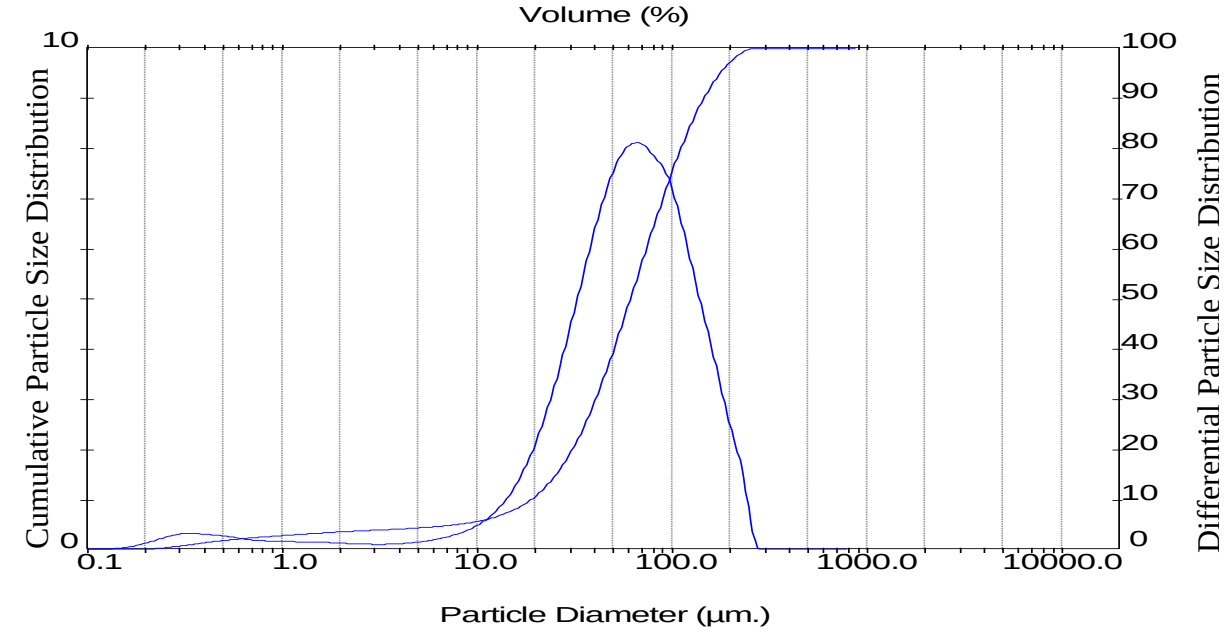

Figure 16: Volumetric particle size distributions of Ef-MCC-sd.

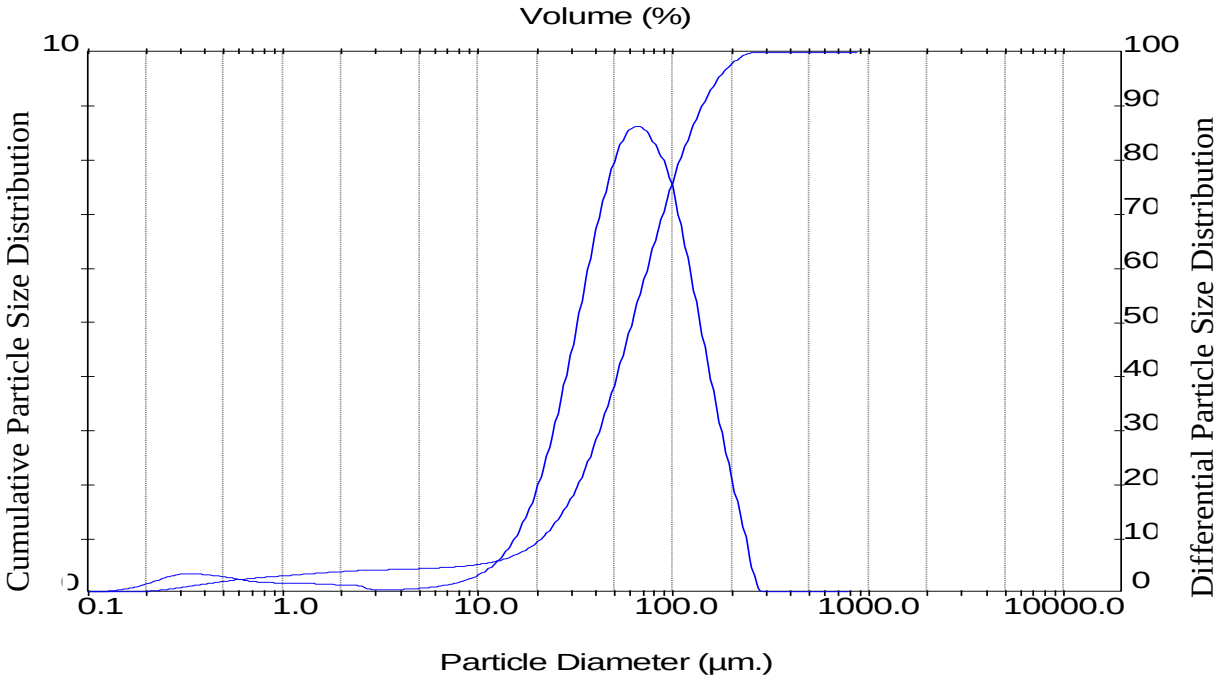

Figure 17: Volumetric particle size distributions of Avicel PH101.

All Ef-MCCs, except Ef-MCC-od, exhibited lower particle size than Avicel PH101 and consequently higher specific surface area (Table 5). The reduced particle size of Ef-MCCs

affects its flowability as a consequence of its increased specific surface area. The exposure of larger surface resulted in resistance to flow of the individual particles (Herting and Kleinebudde, 2007; Thoorens *et al*., 2014). Thus, Ef-MCC powders are predictable to have poor flowability as compared to Avicel PH101. Nevertheless, particle size is not the only factor affecting flow of powders; moisture content, shape and surface charge of particles are known to retard flow properties of powders. Relative span is the measurement of the width of the distribution which is measured as the ratio of the difference of M_{90} and M_{10} to M_{50} where, $M_{10,}$ M_{50} and M_{90} represent 10, 50 and 90 cumulative percent undersize, respectively. A smaller span means narrower particle size distribution. Accordingly, Ef-MCC-sd was found to have slightly narrow particle size distribution relative to Ef-MCC-od and Ef-MCC-mod. However, Ef-MCC-sd exhibited close width of particle size distribution to Avicel PH101.

Table 5: Particle size and size distribution of Ef-MCC and Avicel PH101.

Parameters	Ef-MCC			Avicel PH101
	Ef-MCC-od	Ef-MCC-mod	Ef-MCC-sd	
Avg. Particle size (µm)	79.87 ± 0.7	57.09 ± 0.4	62.84 ± 0.5	71.33 ± 0.9
M_{10} (µm)	20.52 ± 0.61	15.47 ± 0.38	18.98 ± 0.44	19.9 ± 0.53
M_{50} (µm)	54.07 ± 1.3	48.1 ± 1.01	52.72 ± 1.12	59.96 ± 1.6
M_{90} (µm)	151.53 ± 3.02	128.75 ± 2.3	130.01 ± 3.1	143.76 ± 2.61
SSA	0.41 ± 0.012	0.48 ± 0.031	0.46 ± 0.011	0.44 ± 0.014
Relative Span	2.42 ± 0.96	2.36 ± 0.13	2.11 ± 0.09	2.06 ± 0.87

M_{10}, M_{50} and M_{90} represent 10, 50 and 90 cumulative percent undersize, respectively, SSA-specific surface area.

5.4.8. Density and related properties

The powder bulk density, tapped density, true density and related properties are given in Table 6. Bulk and tapped densities give an understanding on the packing arrangement of particles and the compaction profile of a material. The bulk density of a powder defines its packing behavior during the various unit operations of tableting such as die filling, mixing and compression. Higher bulk density is advantageous in tableting due to reduction in the fill volume of the die (Okunlola and Odeku, 2009). On the other hand, lower density facilitates compressibility, i.e.,

the densification of a powder bed due to the application of a stress (Patel *et al*., 2006). The improved compressibility of plastically deforming materials, such as MCC, might then result in improved tabletability as a result of the increased bonding surface area (Abdel-Hamid *et al*., 2011). Low bulk density MCCs have a higher dilution potential and may better counteract the poor tableting properties of APIs (Ponni *et al.*, 2012). Therefore, a decrease in bulk density improves tabletability; however, it might often hamper flowability (Sonnergaard, 2006). In general, the higher the bulk and tapped densities, the better the potential for a material to flow and to rearrange under compression (Kothari *et al.,* 2002).

In the present study, the bulk density of Ef-MCC-od and Ef-MCC-sd were found to be lower than the bulk density of Avicel PH101($p<0.05$); while, the bulk density of Ef-MCC-mod was found to have nearly similar bulk density ($p>0.05$) with Avicel PH101 as clearly indicated in Table 6. On the other hand, the bulk density of Ef-MCC-sd was lower than the bulk density of Ef-MCC-mod ($p <0.05$). Spray-drying converts a liquid into powder producing fine or agglomerated powders, usually approximately spherical with a narrow size range and generally hollow. The hollow nature imparts low bulk density to powders (Di Martino.*et al*., 2001). Thus, the spray drying is expected to create hollow particles and the lower value of bulk density of Ef-MCC-sd powder might be due to this hollow nature. The reduced bulk density of Ef-MCC-od might be due to packing arrangement of particles. If particles are arranged in such a way that they leave large gaps between their surface resulting in low bulk density.

As shown in Table 6, Hausner ratio values of Ef-MCC products were higher compared to the Hausner ratio value of Avicel PH101($p<0.05$). Hausner ratio and Carr's index have been widely used to estimate the flow properties of powders and calculated from bulk and tapped densities. They are considered as indirect measurement of powder flowability (Amin *et al*., 2014). The Hausner ratio value of 1.00–1.11, 1.12–1.18, 1.19–1.25, 1.26–1.34, 1.35–1.45 represent excellent, good, fair, passable and poor flow properties, respectively. Accordingly, these results indicated poor flowability of all prepared Ef-MCCs in contrary to Avicel PH101 which was passable as per the result of the present study. On the other hand, depending on Carr's index value, powder flow character is classified as excellent (≤10%), good (11–15%), fair (16–20%), passable (21–25%), poor (26–31%) and very poor (32–37%) (USP 30/NF 25, 2007). All Ef-MCC products had the Carr's index value in the range of 26–31% which is considered as poor

powder flow and this result was also in line with Hausner ratio. In contrast, the CI of Avicel PH101 lies in 21–25%(passable).

The true density of Ef-MCC-od and Ef-MCC-sd were comparable to that of Avicel PH101($p>0.05$) while the value was significantly lower for Ef-MCC-mod ($P< 0.05$). The lower value of true density of Ef-MCC-mod might be ascribed to lower degree of crystallinity of Ef-MCC-mod. According to Kambli *et al.*, (2017), there is a direct correlation between the degree of crystallinity of cellulose and its true density when determined in a non-polar liquid. The greater the degree of crystallinity, the greater will be the true density of the material. The true density of a 100% crystalline natural cellulose is between 1.582 and 1.599 (Sun, 2005). Since the crystallinity of MCC is noticeably less than 100%, the true density of all Ef-MCCs is expected to be lower than 1.582.

Table 6: Comparison of powder densities and related properties of Ef-MCC-od, Ef-MCC-mod, Ef-MCC-sd and Avicel PH101.

Powder Properties	Ef-MCC-od	Ef-MCC-mod	Ef-MCC-sd	Avicel PH101
Bulk density (g/cm^3)	0.24 ± 0.00	0.33 ± 0.01	0.27 ± 0.02	0.35 ± 0.01
Tapped density (g/cm^3)	0.34 ± 0.01	0.44 ± 0.03	0.38 ± 0.09	0.46 ± 0.06
True density (g/cm^3)	1.574 ± 0.02	1.52 ± 0.012	1.566 ± 0.02	1.58 ± 0.01
Hausner ratio	1.40 ± 0.02	1.38 ± 0.03	1.37 ± 0.02	1.31 ± 0.01
Carr's index (%)	28.40 ± 1.64	27.44 ± 2.0	26.70 ± 1.3	23.74 ± 1.1

Mean ± SD (n=3)

5.4.9. Compressibility Properties of Enset Fiber Microcrystalline Cellulose

Compressibility is the ability of powder bed to form mechanically strong tablet. The mechanically properties (i.e., crushing strength, tensile strength, friability and disintegration time) of plain tablets produced from Avicel PH101 and Ef-MCCs are given in Table 7. The crushing strength and friability test were performed to confirm whether the prepared tablets withstand the physical force during transportation (Setu *et al*, 2015). The crushing strength of

tablets made from Ef-MCCs and Avicel PH101 were in the order of Avicel PH101 tablets >Ef-MCC-sd > Ef-MCC-mod at all levels of compression force. The differences in bulk densities of powders might have resulted in variations in crushing strength as powder with higher bulk density produce harder tablets and vice versa. Usually, higher density MCC tablets have higher mechanical properties. However, not only the differences in bulk densities but also, the difference in DP might bring about difference in crushing strength. According to literature evidence, crushing strength generally increases with decreased DP powder (Iida *et al*., 1997). This is because, DP has a major impact on compressibility of MCC. Cellulose powder with high DP was less compressible than the low DP cellulose powder (Iida *et al*., 1997; Edge *et al.*, 2000; El-Sakhawy and Hassan, 2007; Medina and Kumar, 2007). Ef-MCCs have higher DP compared to Avicel PH101. The difference in crystallinity could also result in difference in tablet hardness. Tensile strength, which is often used to describe strength of a tablets, increased with crushing strength of tablet (Iida *et al*., 1997; Edge *et al.*, 2000; El-Sakhawy and Hassan, 2007). The higher tensile strength is also associated with higher crystallinity of MCC (Jahan *et al*., 2011; Chen *et al*., 2015). Thus, due to the aforementioned reasons, Avicel PH101 tablets were expected to have higher crushing and tensile strength compared to the tablets prepared from Ef-MCCs powder.

Friability is a measure of inter-particular cohesiveness in tablets (Gebre-Mariam and Nikolayev, 1993) and it is a method to determine the physical strength of tablets upon exposure to mechanical shock or attrition. Tablets that lose not more than 1 % of their weight in the friability test are usually considered acceptable (BP, 2009). Since inter-particulate cohesiveness increases with an increase in compression force, friability of compacts of Ef-MCCs and Avicel PH101 decreased with an increase in compression force (Table 7). Friability declined with increasing tablet hardness which in turn resulted from increased in compression force and tablet hardness (Shittu *et al*., 2012). Accordingly, tablets produced with Ef-MCCs and Avicel PH101 had acceptable weight losses during the friability test at all levels of compression force.

The disintegration test indicates the time required for a tablet to break into many small particles having a greater total surface than the intact tablet under specific controlled conditions. It is one of several important tests used for quality control of these dosage forms (Parrott, 1989).

In this work, the disintegration time increased with increased compression force for all compacts. Avicel PH101 showed prolonged disintegration time than both Ef-MCC-mod and Ef-MCC-sd. This was expected as tablets produced from Avicel PH101 were harder at all levels of compression force.

Table 7: Crushing strength, tensile strength, friability and disintegration time of plain tablets of Ef-MCCs and Avicel PH101.

Samples	Parameters	Compression Forces				
		F_{50}	F_{75}	F_{100}	F_{125}	F_{150}
Ef-MCC-sd	CS (N)	43 ± 2.3	63 ± 2.1	84.3 ± 3.4	107 ± 2.8	131 ± 3.2
	Friability (%)	0.7 ± 0.05	0.31 ± 0.01	0.19 ± 0.004	0.15 ± 0.001	0.08 ± 0.009
	DT (in min)	0.43 ± 0.01	0.82 ± 0.03	1.38 ± 0.1	1.62 ± 0.2	5.44 ± 0.20
	TS (Kg/cm^2)	3.81 ± 0.3	7.11 ± 0.5	10.1 ± 0.6	12.2 ± 0.2	15.43 ± 0.9
Ef-MCC-mod	CS (N)	34 ± 3.5	55.2 ± 2.5	76.6 ± 3.0	102 ± 2.8	120.3 ± 2.3
	Friability (%)	1.0 ± 0.06	0.45 ± 0.04	0.2 ± 0.01	0.16 ± 0.1	0.12 ± 0.02
	DT (in min)	0.38 ± 0.02	0.65 ± 0.001	1.2 ± 0.04	1.5 ± 0.05	4.58 ± 0.16
	TS (Kg/cm^2)	3.98 ± 0.4	6.51 ± 0.4	9.83 ± 0.7	11.5 ± 0.3	14.17 ± 0.9
Avicel PH101	CS (N)	48.2 ± 2.1	74.9 ± 2.7	99.2 ± 2.0	124 ± 3.4	149.2 ± 3.0
	Friability (%)	0.41 ± 0.07	0.2 ± 0.05	0.18 ± 0.003	0.10 ± 0.007	0.06 ± 0.02
	DT (in min)	0.55 ± 0.03	0.69 ± 0.01	1.33 ± 0.1	3.7 ± 0.22	6.43 ± 0.20
	TS (Kg/cm^2)	4.49 ± 0.40	7.55 ± 0.64	10.8 ± 0.5	13.8 ± 0.5	17.9 ± 0.57

F: compression force (N), CS: crushing strength, DT: disintegration time, TS: tensile strength

5.5. Lubricant Sensitivity

Lubricants are commonly used in tablet formulations to reduce die wall friction during tablet compression and ejection. Among the different lubricants that are utilized in the pharmaceutical industry, magnesium stearate is the most commonly used. Magnesium stearate forms an adsorbed lubricant film around particles during mixing. This results in a decrease in solid–solid contact, including contact between tablet and die wall, hence, reduction in die wall friction. However, the aforementioned lubricant film also interferes with the bonding properties of the particles by acting as a physical barrier. This causes a decrease in compact strength, especially with excessive lubricant amounts and/or prolonged mixing times (Almaya and Aburub, 2008).

The sequence of lubricant sensitivity (most to least) of Ef-MCCs and Avicel PH101 was as following: Avicel PH101> Ef-MCC-sd> Ef-MCC-mod as assessed from the LSR (Table 8). The more LSR value approaches 1, the more the dry binder is sensitive to lubricant from the viewpoint of decreased strength of compacts (Almaya and Aburub, 2008).

Both Ef-MCC-sd and Ef-MCC-mod were shown to be less lubricant sensitive than Avicel PH101. The reason could have been due to the difference in flowability (Doelker *et al*., 1995). Powder with poor flowability is known to be less lubricant sensitive (Almaya and Aburub, 2008; Gamble *et al.*, 2011). This finding also well agreed with poor flow properties of Ef-MCC-mod and Ef-MCC-sd.

Table 8: The lubricant sensitivity ratio values of Ef-MCC and Avicel PH101.

Samples	Ef-MCC-mod	Ef-MCC-sd	Avicel PH101
LSR	0.10 ± 0.01	0.142 ± 0.004	0.189 ± 0.03

Mean ± SD (n = 3)

5.6. Drug-Excipient Compatibility Study

Drug-excipient interactions/incompatibilities are major concerns in formulation development. The compatibility studies were conducted to evaluate interaction between paracetamol and Ef-MCCs.

FTIR spectrum for pure paracetamol powder is shown in Figure (18). The spectrum displayed specific absorption bands. The assignment of each absorption band is as follows: 3321 cm^{-1}: N–H stretching vibration, 1650 cm^{-1}: C=O stretching vibration and C–N bending vibration, 1608 cm^{-1}: C=C stretching vibration, 1562 cm^{-1}: N–H in-plane bending (or amide II band stretching), 1509 and 1442 cm^{-1}: aromatic ring mode, 1323 cm^{-1}: O–H bending vibration and 1222 cm^{-1}: C–O and/or C–N stretching vibrations (Wang *et al*., 2002; Martínez *et al*, 2014). These absorption bands are characteristic of paracetamol and all absorption bands observed in this work for paracetamol agreed with those previously reported. The absorption bands observed for paracetamol and Ef-MCC remained unchanged when compared with the spectrum data of the paracetamol-MCC (P-MCC) mixture (Figure 19). The physical mixtures contained all the principal bands of the two constituents and showed no shifting of the peaks, indicating the stability and compatibility of Ef-MCC with the drug.

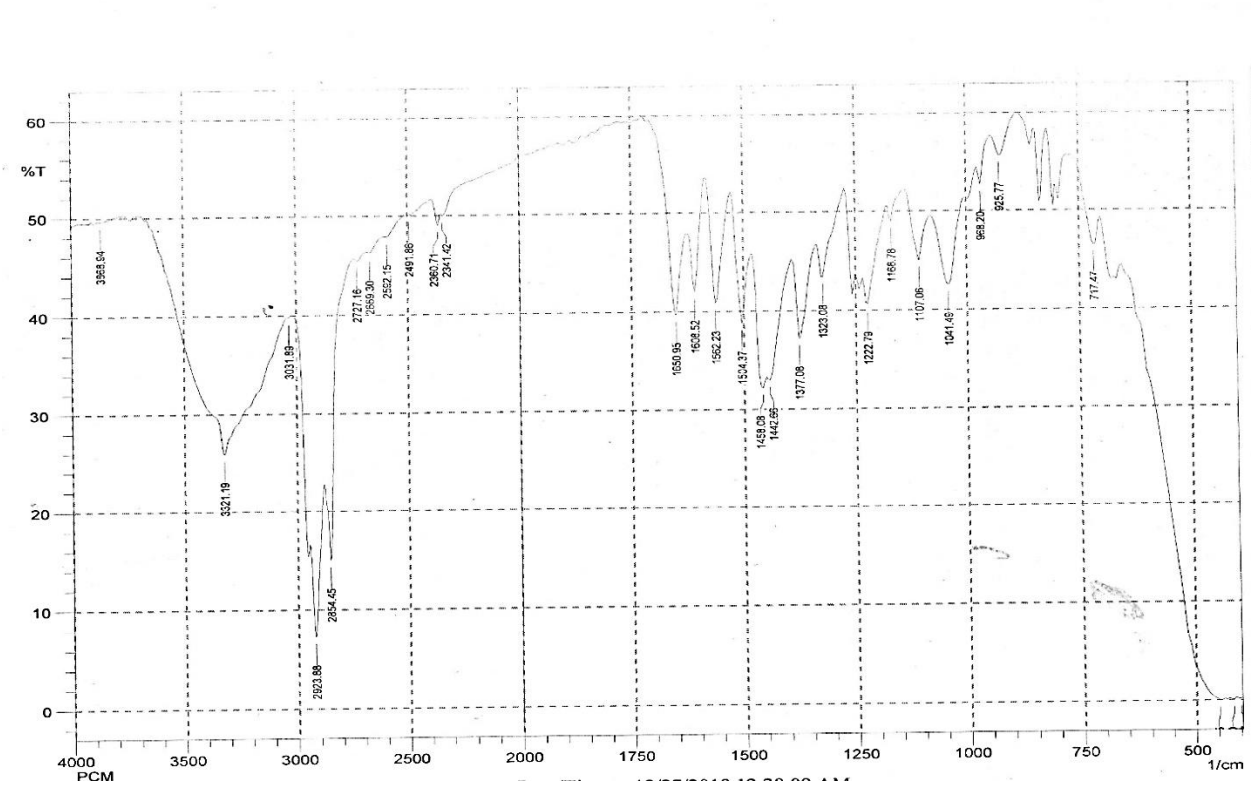

Figure 18: FTIR spectrum of paracetamol.

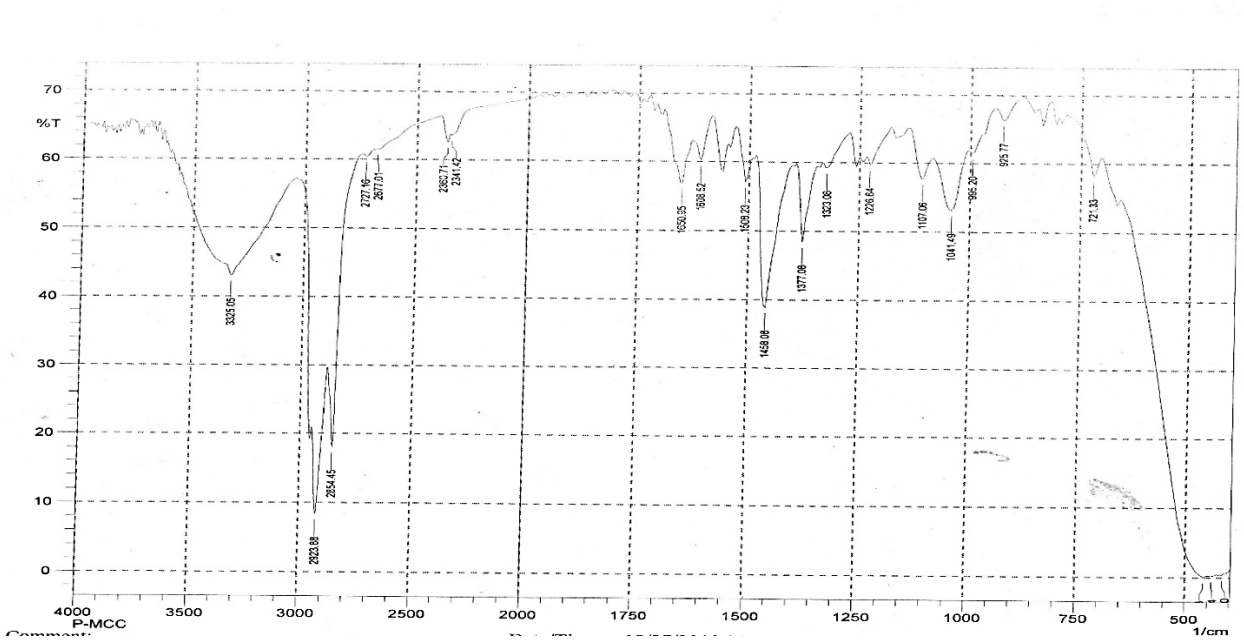

Figure 19: FTIR spectrum of mixture of paracetamol and Ef-MCC-sd.

5.7. Dilution Potential Study

Dilution potential is the amount of poorly compressible drug that can be satisfactorily compressed into a tablet with a directly compressible excipient (Gohel and Jogani, 2005; Olowosulu *et al*., 2014). Paracetamol is a drug widely used in therapeutics for its analgesic and antipyretic properties. Usually, it is formulated in tablets containing 300–500 mg of drug (Martinello *et al.*, 2006). Accordingly, 400 mg of paracetamol tablets were prepared and relationship between amount in percent (%) of paracetamol added to the formulation and tablets mechanical properties were generated to study dilution potential.

5.7.1. Crushing strength, tensile strength and friability

To evaluate the dilution potential of DC excipient, some researchers have suggested friability values of less than 1% as being acceptable for assessing dilution potential. Most commonly, however, dilution potential is assessed by crushing strength and/or tensile strength values together with percent friability (Olowosulu *et al*., 2014).

Crushing strength and tensile strength of paracetamol tablets are given in Table 9. The results displayed a significant decrement in values of the crushing strength ($p<0.05$) as the

concentration of paracetamol increased in tablets produced with different Ef-MCCs and Avicel PH101 as diluents. This might be caused by poor compressibility and elastic recovery of paracetamol (Gohel and Jogani, 2005; Olowosulu *et al*., 2014)**.** This in turn affected tensile strength and percent friability. Accordingly, Tensile strength significantly decreased ($p<0.05$) while friability increased significantly with increased concentration of paracetamol ($p<0.05$).

From the results obtained, one can see that Ef-MCC-sd and Avicel PH101 were able to accommodate paracetamol up to 65% with acceptable tablet mechanical properties i.e., crushing strength of > 40 N and friability <1%. For uncoated immediate release tablet, a crushing strength of about 40-80 N is considered the minimum requirement for a satisfactory tablet (Allen *et al*., 2013; Nkemakolam and Ifeanyi, 2017). Up to 65% paracetamol, Ef-MCC-sd and Avicel PH101 did not show significant difference in crushing strength ($P>0.05$). On the other hand, Ef-MCC-mod was successfully accommodating 50% paracetamol with acceptable crushing strength and percent friability. But the variation was statistically significant with crushing strength of Avicel PH101 tablet. Moreover, blending of 65% or more paracetamol with Ef-MCC-mod resulted tablets with unacceptable crushing strength. This is an exciting outcome about auspicious dilution potential of both Ef-MCC-sd and Ef-MCC-mod.

Many authors studied the plasto-elastic behavior of paracetamol-MCC mixtures and pointed out the optimum concentration of MCC as ranging between 25 and 50% in order to compressed into satisfactory tablets as far as crushing strength, friability and capping tendency were concerned (Bangudu and Pilpel, 1985; Yu *et al.*, 1988; Nada and Graf, 1998). Capping occurred when the amount of Avicel PH101 fell below 25% w/w. This was also confirmed in the present study that tablets had friability >1% (Table 9) for Ef-MCC and Avicel PH101 with 20% w/w in paracetamol. The low crushing strength values coupled with poor compressibility of paracetamol attributed to high friability of tablets containing 80% of paracetamol formulations.

Table 9: Crushing strength, tensile strength and friability of paracetamol tablets.

Samples	Tablet properties	Paracetamol concentration (%) in formulation			
		35	50	65	80
Ef-MCC-mod	CS (N)	62.7 ± 2.51	43.3 ± 3.06	30.7 ± 2.86	15.6 ± 2.16
	TS (Kg/cm^2)	6.74 ± 0.31	4.17 ± 0.31	3.50 ± 0.14	2.25 ± 0.21
	Friability (%)	0.36 ± 0.035	0.71 ± 0.024	0.88 ± 0.02	1.5 ± 0.045
Ef-MCC-sd	CS (N)	68.3 ± 3.5	50 ± 4.05	41.6 ± 2.83	17.3 ± 1.65
	TS (Kg/cm^2)	8.49 ± 0.81	6.22 ± 0.34	4.34 ± 0.62	2.26 ± 0.12
	Friability (%)	0.33 ± 0.035	0.46 ± 0.04	0.83 ± 0.027	1.43 ± 0.039
Avicel PH101	CS (N)	75.6 ± 3.8	55.50 ± 1.9	46 ± 2.3	20.3 ± 2.4
	TS (Kg/cm^2)	9.22 ± 0.31	6.89 ± 0.33	4.46 ± 0.25	2.50 ± 0.33
	Friability (%)	0.21 ± 0.03	0.43 ± 0.05	0.55 ± 0.051	1.41± 0.065

Mean ± SD (n = 10), CS: crushing strength, TS: tensile strength.

5.8. Weight Variation and Thickness

The weight variation and thickness of tablets formulated by direct compression method is summarized in Table 10. The tablets are within acceptable range of weight variation (±5%) which is the limit of the percentage deviation allowed by BP (2009) for tablets weighing 250 mg or more. There was a minor variation in tablet thickness between the different batches of Ef-MCCs and Avicel PH101 formulations. This variation might be related to the variation in powders density and compaction behavior of powder. One important factor among the others that can affect the thickness of a tablet is the compaction characteristics of the material (Allen *et al*., 2013). However, tablet thickness of all the formulations did not show significant difference ($p > 0.05$).

Table 10: Weight and thickness of paracetamol tablets formulated by direct compression method at different paracetamol concentrations.

Samples	Parameters	Paracetamol concentration (%) in formulation			
		35	50	65	80
Ef-MCC-mod	Weight	391 ± 2.33	390.6 ± 4.22	391 ± 4.73	394.2 ± 2.04
	Thickness	4.89 ± 0.02	4.92 ± 0.01	4.93 ± 0.04	4.95 ± 0.03
Ef-MCC-sd	Weight	391.8 ± 2.54	391.2 ± 2.14	391.2 ± 4.71	390.4 ± 4.3
	Thickness	4.89 ± 0.01	4.90 ± 0.03	4.92 ± 0.02	4.94 ± 0.01
Avicel PH101	Weight	390.6 ± 2.82	391.4 ±3.61	391.2 ± 3.97	392 ± 4.34
	Thickness	4.88 ± 0.01	4.89 ± 0.01	4.91 ± 0.03	4.93 ± 0.05

Mean ± SD (n = 20)

5.9. Disintegration Time

The impact of concentration of paracetamol on the disintegration time of tablets is depicted in Figure 20. All paracetamol tablet formulations showed rapid disintegration. Tablets based on Avicel PH101 disintegrated in about 2 min while those made from Ef-MCC-mod and Ef-MCC-sd disintegrated even earlier. This finding indicated the ability of Ef-MCCs to form satisfactorily hard tablets and yet possess unusual short disintegration times. Additionally, the disintegration time of the tablets diminished as the paracetamol concentration increased. Reduction of disintegration time might be explicated on the base of tablet weakness as paracetamol concentration increased and the results agree well with those of the crushing strength of tablets. Generally, the disintegration time is related to hardness i.e. disintegration time increased with increased tablet hardness (Kitazawa *et al*., 1975). In this study, the disintegration times of all paracetamol tablets were much lower than the Pharmacopeial limit (<15 min) (USP 30/NF 25, 2007).

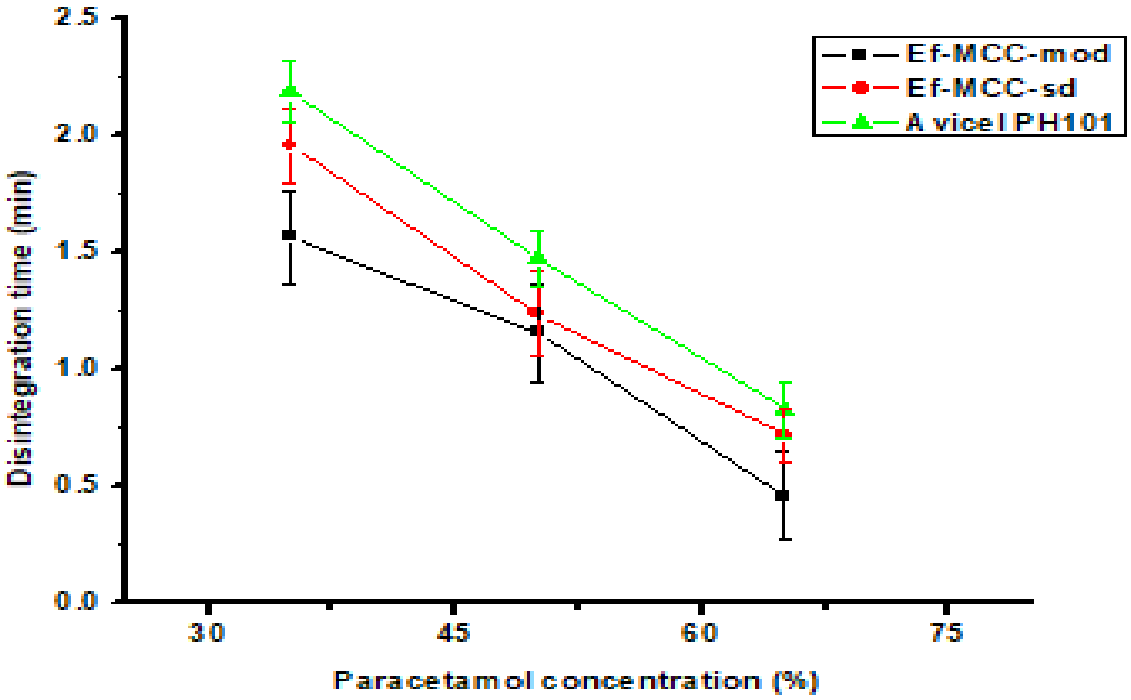

Figure 20: Disintegration time of tablets formulated from Ef-MCC-mod, Ef-MCC-sd and Avicel PH101 at different concentrations of paracetamol.

5.10. Calibration Curve of Paracetamol

The absorbance versus concentration of the solutions was plotted and a calibration curve with a linear regression equation of: Y = 0.056X - 0.011 was found where Y is the absorbance and X is the concentration in µg/ml (Figure 21). The correlation coefficient (r^2) of 0.9996 was obtained indicating a good correlation between the concentration and absorbance.

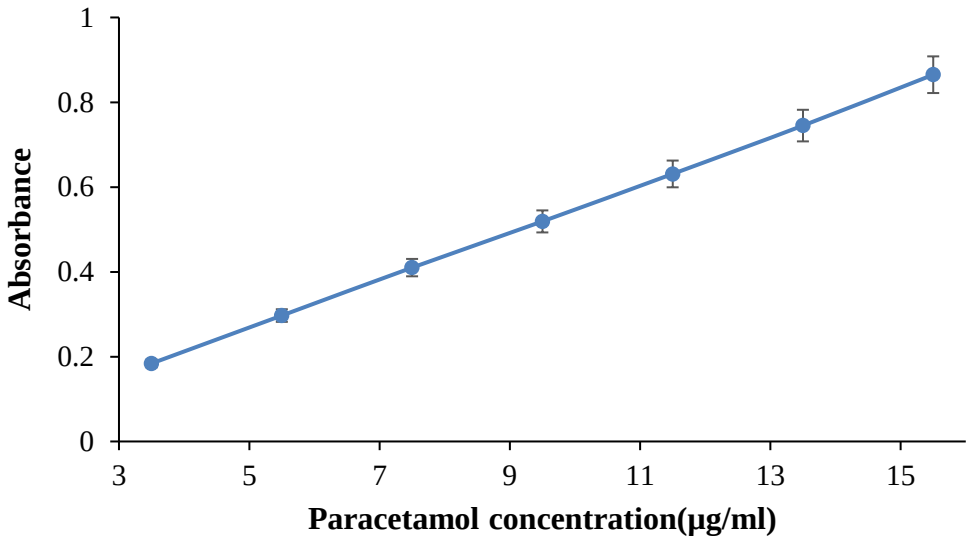

Figure 21: Absorbance of paracetamol in phosphate buffer (pH 5.8) at 243 nm with 95% confidence level.

5.11. *Invitro* Drug Release

Drug dissolution testing is a critical component of pharmaceutical development and manufacturing. The design of new formulations is often guided and assessed based on *invitro* dissolution rates. The dissolution test is used for measuring the time required for a given percentage of the drug substance in a tablet to go into solution under a specified set of conditions in an *invitro* test (Baxter *et al*, 2005). It is an essential tool to evaluate drug release from a dosage form which gives an overview of the drug release in the biological system of the gastro intestinal tract (Olowosulu *et al*., 2017). Figure 22 shows the dissolution rate of the paracetamol tablets (35%, 50%, 65% and 80% w/w) produced from Ef-MCC-sd and Ef-MCC-mod and Avicel PH101. Ef-MCC-mod tablets with 35% paracetamol released 83.7% of the drug at 30 min of dissolution whereas Ef-MCC-sd and Avicel PH101 tablets released 85.6% and 89.9% of the drug at the same concentration of paracetamol, respectively. The amount of paracetamol released from the tablets within 30 min of dissolution increased as paracetamol concentration increased. This might be attributed to reduction of tablet hardness thereby resulted in faster dissolution rate. All formulations fulfilled the specification of the USP 30/NF 25 (2007) i.e. > 80% of the tablet content should be released within 30 min.

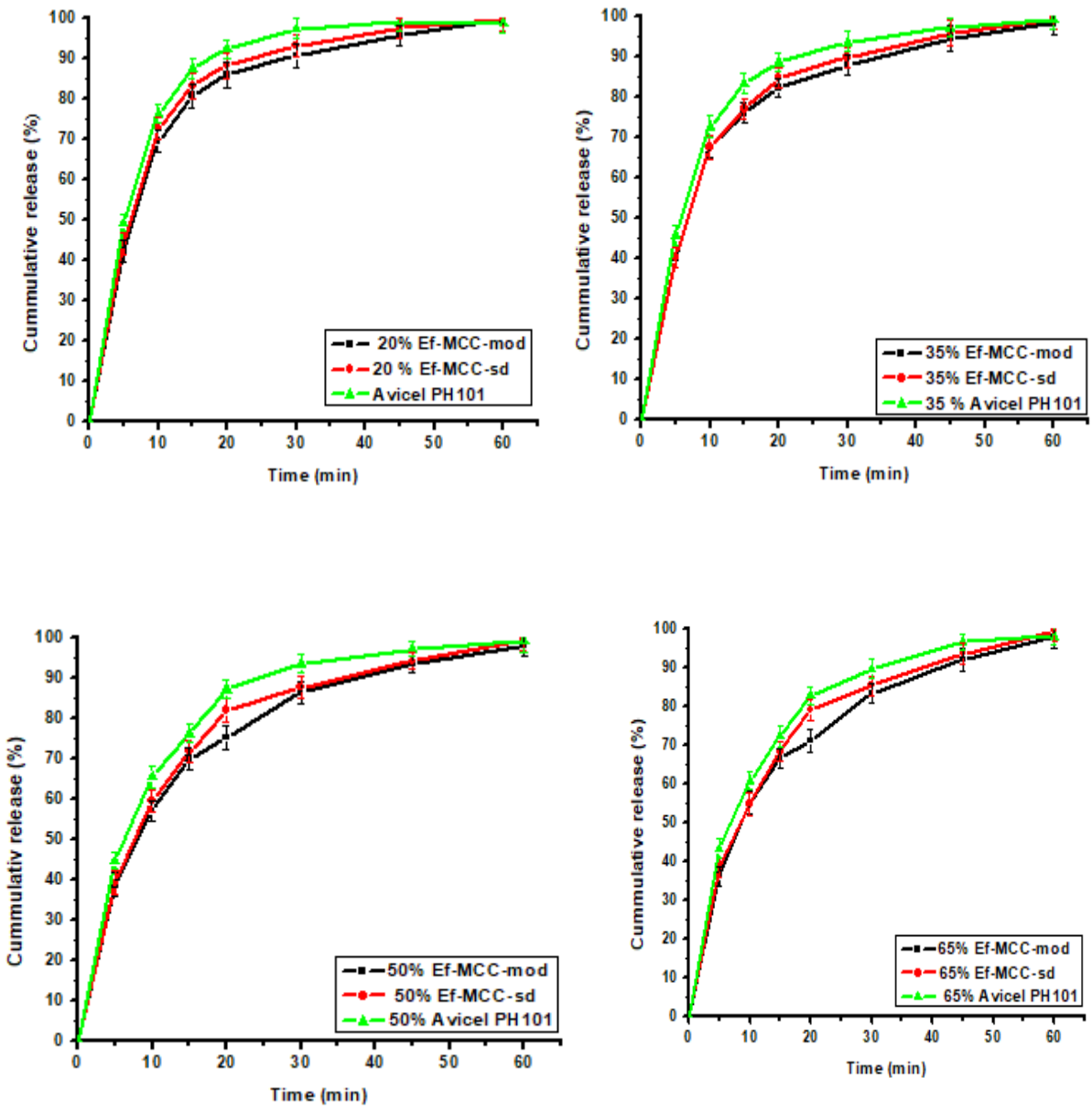

Figure 22: Dissolution profiles of paracetamol tablets containing 20%, 35%, 50% and 65% of Ef-MCC-mod, Ef-MCC-sd and Avicel PH101.

CONCLUSIONS

Cellulose was successfully extracted from enset fiber. Enset fiber is the promising source of cellulose and MCC due to it high yielding potential. All Ef-MCC-od, Ef-MCC-mod and Ef-MCC-sd have DP within Pharmacopeial limit. FT-IR spectra verified the Ef-C and Ef-MCCs have similar typical absorption band of cellulose and Avicel PH101. X-ray diffraction showed Ef-MCCs have comparable crystallinity index to that of Avicel PH101. Particle size analysis also revealed that Ef-MCC exhibited normal particle distribution with lower mean diameter, except Ef-MCC-od, in comparison to Avicel PH101.

There was no significant difference in powder moisture content between Ef-MCCs and Avicel PH101; moisture sorption between Ef-MCC-sd and Avicel PH101. However, Ef-MCCs show slightly lower bulk densities, higher Hausner ratio and Carr's index indicating relatively poor flow in comparison to Avicel PH101. Ef-MCCs also known to have less lubricant sensitivity than Avicel PH101.

Regarding to dilution potential, Ef-MCC-sd were able to accommodate paracetamol up to 65% whereas Ef-MCC-mod was found to accommodate 50% paracetamol with acceptable crushing strength and friability at fixed compression force. Disintegration time and dissolution studies of paracetamol tablets made from Ef-MCCs and Avicel PH101 also found to fall within specified acceptable Pharmacopeial limit.

Based on pertinent findings of this study, the physicochemical properties and dilution potential of Ef-MCCs (particularly Ef-MCC-sd) and Avicel PH101 were almost similar. Therefore, it is possible to conclude that Ef-MCCs can be considered as alternative DC excipient to Avicel PH101 in tablet formulations.

SUGGESTIONS FOR FURTHER STUDY

The results of this study provided an insight into some physicochemical properties and direct compressibility of Ef-MCC. However, the following issues were uncovered. Therefore, based on promising results of this study, the followings are suggested for further investigation.

- Evaluate the deformation characteristics of Ef-MCC (Heckle analysis);
- Evaluate of MCC as a diluent in tablets prepared by wet granulation as well as a filler for capsules and spheres; and
- Explore the use of cross-linked Ef-MCC as sustaining release excipient and its application in extrusion spherization.
- Accelerated and long-term stability studies

REFERENCES

Abdel-Hamid, S., Alshihabi, F. and Betz, G., 2011. Investigating the effect of particle size and shape on high speed tableting through radial die-wall pressure monitoring. *Int. J. Pharm.*, **413**, 29-35.

Adel, A.M., El–Wahab, Z.H.A., Ibrahim, A.A. and Al–Shemy, M.T., 2010. Characterization of microcrystalline cellulose prepared from lignocellulosic materials. Part I. Acid catalyzed hydrolysis. *Bioresour. Technol.,* **101**, 4446-4455.

Adel AM, El-Wahab ZH, Ibrahim AA, Al-Shemy MT., 2011. Characterization of microcrystalline cellulose prepared from lignocellulosic materials. Part II: Physicochemical properties. *Carbohydr. Polym.,* **83**, 676-87.

Albers, J., Knop, K., Kleinebudde, P., 2006. Brand-to-brand and batch-to-batch uniformity of microcrystalline cellulose in direct tableting with a pneumo-hydraulic tablet press. *Pharm. Ind.,* **68**, 1420–1428.

Alemdar, A. and Sain, M., 2008. Isolation and characterization of nanofibers from agricultural residues–Wheat straw and soy hulls. *Bioresour. Technol*., **99**, 1664-1671.

Allen, L.V, Popovich, N.G., Ansel, H.C., 2013. Ansel's pharmaceutical dosage forms and drug delivery systems, 9th Edition, Lippincott Williams and Wilkins, Philadelphia. P. 233

Almaya, A. and Aburub, A., 2008. Effect of particle size on compaction of materials with different deformation mechanisms with and without lubricants. *Aaps Pharm Scitech.*, **9**, 414-418.

Amin, M.C.I.M., Abadi, A.G. and Katas, H., 2014. Purification, characterization and comparative studies of spray-dried bacterial cellulose microparticles. *Carbohydr. Polym.,* **99**, 180-189.

Amin, F.R., Khalid, H., Zhang, H., u Rahman, S., Zhang, R., Liu, G. and Chen, C., 2017. Pretreatment methods of lignocellulosic biomass for anaerobic digestion. *AMB Express*, **7**, 72.

Bangudu, A.B. and Pilpel, N., 1985. Effects of composition, moisture and stearic acid on the plasto-elasticity and tableting of paracetamol-microcrystalline cellulose mixtures. *J. Pharm. Pharmacol., **37**,* 289-293.

Battista, O.A., 1950. Hydrolysis and crystallization of cellulose. *Ind. Eng. Chem., **42***, 502-507

Battista, O.A. and Smith, P.A., 1962. Microcrystalline cellulose. *Ind. Eng. Chem.*, **54**, 20-29.

Baxter, J.L., Kukura, J. and Muzzio, F.J., 2005. Hydrodynamics-induced variability in the USP apparatus II dissolution test. *Int. J. Pharm.*, **292**, 17-28.

Beten, D.B., Yüksel, N. and Baykara, T., 1994. The changes in the mechanic properties of a direct tableting agent microcrystalline cellulose by precompression. *Drug Dev. Ind. Pharm.*, **20**, 2323-2331.

Bhattacharya, D., Germinario, L.T. and Winter, W.T., 2008. Isolation, preparation and characterization of cellulose microfibers obtained from bagasse. *Carbohydr. Polym.*, **73**, 371-377.

Bhimte, N.A. and Tayade, P.T. 2007. Evaluation of microcrystalline cellulose prepared from sisal fibers as a tablet excipient: a technical note. *AAPS Pharm. Sci. Technol*, **8**, 1-6

Bochek, A.M., 2003. Effect of hydrogen bonding on cellulose solubility in aqueous and nonaqueous solvents. *Russ. J. Appl. Chem.*, **76**, 1711-1719.

BP, 2009. British Pharmacopoeia, The Stationery Office on behalf of the Medicines and Healthcare products Regulatory Agency (MHRA), London, Vol. I & II.

Carrier, M., Loppinet-Serani, A., Denux, D., Lasnier, J.M., Ham-Pichavant, F., Cansell, F. and Aymonier, C., 2011. Thermogravimetric analysis as a new method to determine the lignocellulosic composition of biomass. *Biomass and Bioenergy*, **35**, 298-307.

Cheng, Y.S., Zheng, Y., Yu, C.W., Dooley, T.M., Jenkins, B.M. and VanderGheynst, J.S., 2010. Evaluation of high solids alkaline pretreatment of rice straw. *Appl. Biochem. Biotechnol.*, **162**, 1768-1784.

Chieng, B.W., Lee, S.H., Ibrahim, N.A., Then, Y.Y. and Loo, Y.Y., 2017. Isolation and Characterization of Cellulose Nanocrystals from Oil Palm Mesocarp Fiber. *Polym.*, **9**, 355.

Chirayil, C.J., Joy, J., Mathew, L., Mozetic, M., Koetz, J. and Thomas, S., 2014. Isolation and characterization of cellulose nanofibrils from Helicteres isora plant. *Ind. Crops Prod.*, **59**, 27-34.

Chuayjuljit, S., Su-uthai, S. and Charuchinda, S., 2010. Poly (vinyl chloride) film filled with microcrystalline cellulose prepared from cotton fabric waste: properties and biodegradability study. *Waste Manage. Res.,* **28**, 109-117.

Costa L. A. D., Ananda F. F, Fabiano V. P., Janice I. D., 2013. Extraction and Characterization of Cellulose Nanocrystals from Corn Stover. *Cellulose Chem.Technol.,* **49**, 127-133.

Das, K., Ray, D., Bandyopadhyay, N.R. and Sengupta, S., 2010. Study of the properties of microcrystalline cellulose particles from different renewable resources by XRD, FTIR, nanoindentation, TGA and SEM. *J. Polym. Environ.,* **18**, 355-363.

Deepa, B., Abraham, E., Koshy, R.R., Pothan, L.A. and Thomas, S., 2015. Extraction and characterization of cellulose nanofibers from banana plant. In: Handbook of Polymer Nanocomposites. Processing, Performance and Application. Springer, Berlin, Heidelberg, pp. 65-80.

Deraman, M., Zakaria, S. and Murshidi, J.A., 2001. Estimation of crystallinity and crystallite size of cellulose in benzylated fibres of oil palm empty fruit bunches by X-ray diffraction. *Jpn. J. of Appl. Phys., **40***, 3311.

De Menezes, A.J., Siqueira, G., Curvelo, A.A. and Dufresne, A., 2009. Extrusion and characterization of functionalized cellulose whiskers reinforced polyethylene nanocomposites. *Polym*., **50**, 4552-4563.

Di Martino, P., Scoppa, M., Joiris, E., Palmieri, G.F., Andres, C., Pourcelot, Y. and Martelli, S., 2001. The spray drying of acetazolamide as method to modify crystal properties and to improve compression behaviour. *Int. J. Pharm.*, **213**, 209-221.

Doelker, E., Massuelle, D., Veuillez, F. and Humbert-Droz, P., 1995. Morphological, packing, flow and tableting properties of new Avicel types. *Drug Dev. Ind. Pharm.,* **21**, 643-661.

Duan, L., Yu, W. and Li, Z., 2017. Analysis of Structural Changes in Jute Fibers after Peracetic Acid Treatment. *J. Eng. Fab. Fib.*, **12**.

Edge, S., Steele, D. F., Chen, A., Tobyn, M. J., & Staniforth, J. N. 2000. The mechanical properties of compacts of microcrystalline cellulose and silicified microcrystalline cellulose. *Int. J. Pharm.,* **200**, 67–72.

Elanthikkal, S., Gopalakrishnapanicker, U., Varghese, S. and Guthrie, J.T., 2010. Cellulose microfibres produced from banana plant wastes: Isolation and characterization. *Carbohydr. Polym.*, **80**, 852-859.

El-Sakhawy, M. and Hassan, M.L., 2007. Physical and mechanical properties of microcrystalline cellulose prepared from agricultural residues. *Carbohydr. Polym.* **67**, 1-10.

Figueiredo, J.A., Ismael, M.I., Anjo, C.M.S. and Duarte, A.P., 2010. Cellulose and derivatives from wood and fibers as renewable sources of raw-materials. In: Carbohydrates in Sustainable Development I, Springer, Berlin, Heidelberg, pp. 117-128.

Gamble, J.F., Chiu, W.S. and Tobyn, M., 2011. Investigation into the impact of sub-populations of agglomerates on the particle size distribution and flow properties of conventional microcrystalline cellulose grades. *Pharm. Dev. Technol.*, **16**, 542-548.

Ganesan, V., Rosentrater, K.A. and Muthukumarappan, K., 2008. Flowability and handling characteristics of bulk solids and powders–a review with implications for DDGS. *Biosyst. Eng.*, **101**, 425-435.

Gbenga, B.L. and Fatimah, O.F., 2014. Investigation of α-Cellulose Content of Sugarcane Scrappings and Bagasse as Tablet Disintegrant. *J. Basic Appl. Sci.*, **10**, 142-148.

Gebre-Mariam, T. and Nikolayev, A.S., 1993. Evaluation of starch obtained from Ensete ventricosum as a binder and disintegrant for compressed tablets. *J. Pharm. Pharmacol.*, **45**, 317-320.

Gebre-Mariam, T., Schmidt, P. C. 1996a. Isolation and physico-chemical properties of enset starch. *Starch/Stärke*, 48, 208 - 214.

Gebre-Mariam, T., Schmidt, P. C. 1996b. Characterization of enset starch and its use as a binder and disintegrant for tablets, *Pharmazie*, **51**, 303 - 311.

Gohel, M.C. and Jogani, P.D., 2005. A review of co-processed directly compressible excipients. *J. Pharm. Sci.*, **8**, 76-93.

Haafiz, M.M., Eichhorn, S.J., Hassan, A. and Jawaid, M., 2013. Isolation and characterization of microcrystalline cellulose from oil palm biomass residue. *Carbohydr. Polym.*, **93**, 628-634.

Habib, Y., Augsburger, L., Reier, G., Wheatley, T. and Shangraw, R., 1996. Dilution potential: a new perspective. *Pharmaceutical development and technology*, ***1***, 205-212.

Herting, M.G. and Kleinebudde, P., 2007. Roll compaction/dry granulation: Effect of raw material particle size on granule and tablet properties. *Int. J. Pharm.*, **338**, 110-118.

Ibrahim, M.M., El-Zawawy, W.K., Abdel-Fattah, Y.R., Soliman, N.A. and Agblevor, F.A., 2011. Comparison of alkaline pulping with steam explosion for glucose production from rice straw. *Carbohydr. Polym.*, **83**, 720-726.

Ibrahim, M.M., El-Zawawy, W.K., Jüttke, Y., Koschella, A. and Heinze, T., 2013. Cellulose and microcrystalline cellulose from rice straw and banana plant waste: preparation and characterization. *Cellulose*, **20**, 2403-2416.

Iida, K., Aoki, K., Danjo, K., Otsuka, A., Chen, C.Y. and Horisawa, E., 1997. A comparative evaluation of the mechanical properties of various celluloses. *Chem. Pharm. Bull*, **45(**1), 217-220.

Jahan, M.S., Saeed, A., He, Z. and Ni, Y., 2011. Jute as raw material for the preparation of microcrystalline cellulose. *Cellulose*, **18**, 451-459.

Jahan, M.S., Rumee, J.N., Rahman, M.M. and Quaiyyum, A., 2014. Formic acid/acetic acid/water pulping of agricultural wastes. *Cellul. Chem. Technol.*, **48**, 111-118.

Jedvert, K. and Heinze, T., 2017. Cellulose modification and shaping–a review. *J. Polym. Eng.*, **37**, 845-860.

John R., Julian A., Manuel H. (2013). Screening of several excipients for direct compression of tablets: A new perspective based on functional properties, *J. Basic and Appl. Pharm. Sci.* **34**, 17-23

Kambli, N.D., Mageshwaran, V., Patil, P.G., Saxena, S. and Deshmukh, R.R., 2017. Synthesis and characterization of microcrystalline cellulose powder from corn husk fibres using bio-chemical route. *Cellulose*, **24**, 5355-5369.

Karande, V.S., Bharimalla, A.K., Hadge, G.B., Mhaske, S.T. and Vigneshwaran, N., 2011. Nanofibrillation of cotton fibers by disc refiner and its characterization. *Fibers Polym.*, **12**(3), 399.

Kim, U.J., Eom, S.H. and Wada, M., 2010. Thermal decomposition of native cellulose: influence on crystallite size. *Polym. Degrad. Stab.*, **95**, 778-781.

Kitazawa, S., Johno, I., Ito, Y., Teramura, S. and Okada, J., 1975. Effects of hardness on the disintegration time and the dissolution rate of uncoated caffeine tablets. *J. Pharm. Pharmacol.*, **27**, 765-770.

Klančnik, G., Medved, J. and Mrvar, P., 2010. Differential thermal analysis (DTA) and differential scanning calorimetry (DSC) as a method of material investigation Diferenčna termična analiza (DTA) in diferenčna vrstična kalorimetrija (DSC) kot metoda za raziskavo materialov. *Materials and Geoenvironment*, **57**, 127-142.

Klemm, D., Heublein, B., Fink, H.P., Bohn, A., 2005. Cellulose:fascinating biopolymer and sustainable raw material. *Angew. Chem. Int. Ed*. **44**, 3358–3393.

Kothari, S.H., Kumar, V. and Banker, G.S., 2002. Comparative evaluations of powder and mechanical properties of low crystallinity celluloses, microcrystalline celluloses, and powdered celluloses. *Int. J. Pharm.*, **232**, 69-80.

Krstic, Marko, Zoran Maksimovic, Svetlana Ibric, Tamara Bakic, Jovana Prodanovic, and Slavica Razic. 2018. "Lignocellulosic Biomass as a Source of Microcrystalline Cellulose–Chemical and Technological Characterization and Future Perspectives." *Cellulose Chem. Technol.*, **52**, 577-588.

Kuentz, M. and Leuenberger, H., 2000. A new theoretical approach to tablet strength of a binary mixture consisting of a well and a poorly compactable substance. *Eur.J.Pharm. Biopharm.*, **49**, 151-159.

Kumar, R., and Wyman, C. E., 2009. "Effects of cellulase and xylanase enzymes on the deconstruction of solids from pretreatment of poplar by leading technologies," *Biotechnol. Prog.*, **25**, 302–314.

Kumar, P., Barrett, D.M., Delwiche, M.J. and Stroeve, P., 2009. Methods for pretreatment of lignocellulosic biomass for efficient hydrolysis and biofuel production. *Ind. Eng. Chem. Res.*, **48**, 3713-3729.

Kushner IV, J., 2013. Utilizing quantitative certificate of analysis data to assess the amount of excipient lot-to-lot variability sampled during drug product development. *Pharm. Dev. Technol.*, **18**, 333-342.

Lemma, H., Zebene, K., Sisay F., Abubeker Y., 2016. Ensete Fiber, Leaf, stem. Lignocellulose **5**, 139-151.

Lin, C., Zhan, H., Liu, M., Fu, S., & Lucia, L. A. 2009. Novel preparation and characterization of cellulose microparticles functionalized in ionic liquids. *Langmuir*, **25**, 10116–10120.

Liu, C.F., Ren, J.L., Xu, F., Liu, J.J., Sun, J.X. and Sun, R.C., 2006. Isolation and characterization of cellulose obtained from ultrasonic irradiated sugarcane bagasse. *J. Agric. Food Chem.*, ***54***(16), 5742-5748.

Liu, W., Fei, M.E., Ban, Y., Jia, A. and Qiu, R., 2017. Preparation and evaluation of green composites from microcrystalline cellulose and a soybean-oil derivative. *Polymers*, ***9***, 541.

Maheswari, C.U., Reddy, K.O., Muzenda, E., Guduri, B.R. and Rajulu, A.V., 2012. Extraction and characterization of cellulose microfibrils from agricultural residue–Cocos nucifera L. *Biomass and bioenergy*, **46**, 555-563.

Maiti, S., Jayaramudu, J., Das, K., Reddy, S.M., Sadiku, R., Ray, S.S. and Liu, D., 2013. Preparation and characterization of nano-cellulose with new shape from different precursor. *Carbohydr. Polym.*, **98**, 562-567.

Maepa, C.E., Jayaramudu, J., Okonkwo, J.O., Ray, S.S., Sadiku, E.R. and Ramontja, J., 2015. Extraction and characterization of natural cellulose fibers from maize tassel. *Int. J. Polym. Anal. Charact.*, **20**, 99-109.

Magule, T. O., B. Tesfaye, M. Catellani and M. Enrico Pè ., 2014. Indigenous knowledge, use and on-farm management of enset (Enseteventricosum (Welw.)Cheesman) diversity in Wolaita, Southern Ethiopia. *J.Ethnobiol. and Ethnomed.*, **10**, 1-18.

Mandal, A. and Chakrabarty, D., 2011. Isolation of nanocellulose from waste sugarcane bagasse (SCB) and its characterization. *Carbohydr Polym.*, **86**, 1291-1299.

Martinello, T., Kaneko, T.M., Velasco, M.V.R., Taqueda, M.E.S. and Consiglieri, V.O., 2006. Optimization of poorly compactable drug tablets manufactured by direct compression using the mixture experimental design. *Int. J. Pharm.*, **322**, 87-95.

Martínez, L.M., Videa, M., López-Silva, G.A., Carlos, A., Cruz-Angeles, J. and González, N., 2014. Stabilization of amorphous paracetamol-based systems using traditional and novel strategies. *Int. J. Pharm.*, **477**, 294-305.

McIntosh, S. and Vancov, T., 2010. Enhanced enzyme saccharification of Sorghum bicolor straw using dilute alkali pretreatment. *Bioresour. Technol.*, **101**, 6718-6727.

Medina, M.D.L.L.R. and Kumar, V., 2007. Comparative evaluation of powder and tableting properties of low and high degree of polymerization cellulose I and cellulose II excipients. *Int. J. Pharm.*, **337**, 202-209.

Mertens, J., 2003. Anselme Payen (1795–1871), Learned Manufacturer of Chemical Products. Ambix, **50**, 182-207.

Mihranyan, A., Llagostera, A.P., Karmhag, R., Strømme, M. and Ek, R., 2004. Moisture sorption by cellulose powders of varying crystallinity. *Int. J. Pharm.*, **269**, 433-442.

Morán, J.I., Alvarez, V.A., Cyras, V.P. and Vázquez, A., 2008. Extraction of cellulose and preparation of nanocellulose from sisal fibers. *Cellulose, **15***.149-159.

Mosier, N., Wyman, C., Dale, B., Elander, R., Lee, Y.Y., Holtzapple, M. and Ladisch, M., 2005. Features of promising technologies for pretreatment of lignocellulosic biomass. *Bioresour. Technol.*, **96**, 673-686.

Nada, A.H. and Graf, E., 1998. Evaluation of Vitacel M80K as a new direct compressible vehicle. *Eur. J. Pharm. Biopharm.*, **46**, 347-353.

Nkemakolam, N. and Ifeanyi, O.S., 2017. Effect of Drying Methods on the Powder and Compaction Properties of Microcrystalline Cellulose Derived from Cocos nucifera. *Br. J. Pharm. Res.*, **20**.

Okunlola A., Odeku O. (2009). Compressional characteristics and tableting properties of starches obtained from four diosco rea species, *Farmacia*, **57**, 6

Oliveira, R.L., da Silva Barud, H., de Assunçao, R.M., da Silva Meireles, C., Carvalho, G.O., Rodrigues Filho, G., Messaddeq, Y. and Ribeiro, S.J.L., 2011. Synthesis and characterization of microcrystalline cellulose produced from bacterial cellulose. *J. Therm Anal Calorim.*, **106**, 703-709.

Olowosulu, A.K., Oyi, A.R., Isah, A.B., Ibrahim, M.A. and Olowosulu, A.K., Dilution Potential and Filler-Binder Functionality of Novel Coprocessed Starch Based Excipients (StarAc) in the Formulation of Metronidazole Tablets. *Nig. J. Pharm. Sci.*, **13**, 44-53

Ouajai, S. and Shanks, R.A., 2005. Composition, structure and thermal degradation of hemp cellulose after chemical treatments. *Polym. Degrad. Stab.*, **89**, 327-335.

Oyeniyi, Y.J. and Achor, M., 2014. The effect of drying techniques on the elastoplastic properties of locally processed microcrystalline cellulose. *Ife J.Sci.*, **16**, 73-80.

Patel, S., Kaushal, A.M. and Bansal, A.K., 2007. Effect of particle size and compression force on compaction behavior and derived mathematical parameters of compressibility. *Pharm. Res.,* **24**, 111-124.

Parrott, E.L., 1989. Comparative evaluation of a new direct compression excipient, Soludex™ 15. *Drug Dev. Ind. Pharm.,* **15**, 561-583.

Podczeck, F. and Révész, P., 1993. Evaluation of the properties of microcrystalline and microfine cellulose powders. *Int. J. Pharm.*, **91**, 183-193.

Poletto, M., Pistor, V., Zeni, M. and Zattera, A.J., 2011. Crystalline properties and decomposition kinetics of cellulose fibers in wood pulp obtained by two pulping processes. *Polym. Degrad. Stab.,* **96**, 679-685.

Pönni, R., Vuorinen, T., Kontturi, E., 2012. Proposed nano-scale coalescence of cellulose in chemical pulp fibers during technical treatments. *Bio. Res.,* **7**, 6077–6108

Rowe, R.C., Sheskey, P.J. and Owen, S.C. eds., 2006. Handbook of pharmaceutical excipients (Vol. 1). London: Pharmaceutical press.

Roy, D., Semsarilar, M., Guthrie, J.T. and Perrier, S., 2009. Cellulose modification by polymer grafting: a review. Chemical Society Reviews, **38**, 2046-2064.

Sassner, P., Galbe, M. and Zacchi, G., 2008. Techno-economic evaluation of bioethanol production from three different lignocellulosic materials. *Biomass Bioenergy*, **32**, 422-430.

Saxena Inder M. and Malcolm, R. B. Jr., 2005. Cellulose Biosynthesis: Current Views and Evolving Concepts. *Annals of Botany,* **96**, 9–21

Setu et al., 2014. Preparation of Microcrystalline Cellulose from Cotton and its Evaluation as Direct Compressible Excipient in the Formulation of Naproxen Tablets. *Dhaka Univ. J. Pharm. Sci.* **13**, 187-192.

Shanmugam N, Nagarkar RD, Kurhade Manisha (2015) Microcrystalline cellulose powder from banana pseudostem fibres using bio-chemical route. *Indian J Nat Prod Resour* **6**, 42–50

Shittu, A.O., Oyi, A.R., Isah, A.B. and Ibrahim, M.A., 2012. Design and Evaluation of a 3-Component Composite Excipient "Microcrystarcellac" as a Filler-Binder for Direct Compression Tabletting and its Utilisation in the Formulation of Paracetamol and Ascor. *Global. J. Med. Res,* **12**.

Sonnergaard, J.M., 2006. Quantification of the compactibility of pharmaceutical powders. *Eur. J. Pharm. Biopharm.*, **63**, 270-277.

Sugiyama, J., Persson, J. and Chanzy, H. 1991a. Combined IR and electron diffraction study of the polymorphism of native cellulose. *Macromolecules,* **24**, 2461–2466.

Sun, C.C., 2005. True density of microcrystalline cellulose. Journal of pharmaceutical sciences, **94**, 2132-2134.

Sun, C.C., 2008. Mechanism of moisture induced variations in true density and compaction properties of microcrystalline cellulose. *Int. J. Pharm.*, **346**, 93-101.

Sun, J.X., Sun, X.F., Zhao, H. and Sun, R.C., 2004. Isolation and characterization of cellulose from sugarcane bagasse. *Polym. Degrad. Stab.*, **84**, 331-339.

Sun, Y. and Cheng, J., 2002. Hydrolysis of lignocellulosic materials for ethanol production: a review. *Bioresour. Technol.*, **83**, 1-11.

Sundar, S., 2011. Chemical modification of cellulose fibers and their orientation in magnetic field (Doctoral dissertation), University of Toronto, Canada.

Suzuki, T. and Nakagami, H., 1999. Effect of crystallinity of microcrystalline cellulose on the compactability and dissolution of tablets. *Eur. J. Pharm. Biopharm.*, **47**, 225-230.

Terinte, N., Ibbett, R. and Schuster, K.C., 2011. Overview on native cellulose and microcrystalline cellulose I structure studied by X-ray diffraction (WAXD): Comparison between measurement techniques. *Lenzinger Ber.*, **89**, 118-131.

Thoorens, G., Krier, F., Leclercq, B., Carlin, B. and Evrard, B., 2014. Microcrystalline cellulose, a direct compression binder in a quality by design environment—A review. *Int. J. Pharm.* **473**, 64-72.

Tibolla, H., Pelissari, F.M. and Menegalli, F.C., 2014. Cellulose nanofibers produced from banana peel by chemical and enzymatic treatment. *Food Sci. Technol.*, **59**, 1311-1318.

Trache, D., Donnot, A., Khimeche, K., Benelmir, R. and Brosse, N., 2014. Physico-chemical properties and thermal stability of microcrystalline cellulose isolated from Alfa fibres. *Carbohydr. polym.*, **104**, 223-230.

USP, U., 2007. 30, NF 25. In: The United States Pharmacopeia and The National Formulary, The United States Pharmacopoeial Convention, INC.

Wang, D., Shang, S.B., Song, Z.Q. and Lee, M.K., 2010. Evaluation of microcrystalline cellulose prepared from kenaf fibers. *J. Ind. Eng. Chem.,* **16**, 152-156.

Wang, S.L., Lin, S.Y. and Wei, Y.S., 2002. Transformation of metastable forms of acetaminophen studied by thermal Fourier transform infrared (FT-IR) microspectroscopy. *Chem. Pharm. Bull.*, **50**, 153-156.

Yang, H., Yan, R., Chen, H., Lee, D.H. and Zheng, C., 2007. Characteristics of hemicellulose, cellulose and lignin pyrolysis. *Fuel*, **86**, 1781-1788.

Yemataw Z., Mohamed H., Diro M. and Addis T. 2014. Enset (Enseteventricosum) clone selection by farmers and their cultural practices in southern Ethiopia. *Genet. Resour. Crop Evol*., **61**, 1091-1104.

Yu, H.C.M., Rubinstein, M.H., Jackson, I.M. and Elsabbagh, H.M., 1988. Multiple compression and plasto-elastic behaviour of paracetamol and microcrystalline cellulose mixtures. *J. Pharm. Pharmacol.* **40**, 669-673.

Zhang, G., Zhang, L., Deng, H. and Sun, P., 2011. Preparation and characterization of sodium carboxymethyl cellulose from cotton stalk using microwave heating. *J. Chem. Technol. Biotechnol*., **86**, 584-589.

Zhao, Y., Wang, Y., Zhu, J.Y., Ragauskas, A. and Deng, Y., 2008. Enhanced enzymatic hydrolysis of spruce by alkaline pretreatment at low temperature. *Biotechnol. Bioeng.* **99**, 1320-1328.

Zhong, C., Wang, C., Huang, F., Jia, H. and Wei, P., 2013. Wheat straw cellulose dissolution and isolation by tetra-n-butylammonium hydroxide. *Carbohydr. Polym.*, **94**, 38-45.